Technology Focus

Electronics/Computers

Software

Materials

Mechanics/Machinery

Manufacturing

Bio-Medical

Physical Sciences

Information Sciences

Books and Reports

INTRODUCTION

Tech Briefs are short announcements of innovations originating from research and development activities of the National Aeronautics and Space Administration. They emphasize information considered likely to be transferable across industrial, regional, or disciplinary lines and are issued to encourage commercial application.

Additional Information on NASA Tech Briefs and TSPs

Additional information announced herein may be obtained from the NASA Technical Reports Server: **http://ntrs.nasa.gov**.

Please reference the control numbers appearing at the end of each Tech Brief. Information on NASA's Innovative Partnerships Program (IPP), its documents, and services is available on the World Wide Web at **http://www.ipp.nasa.gov**.

Innovative Partnerships Offices are located at NASA field centers to provide technology-transfer access to industrial users. Inquiries can be made by contacting NASA field centers listed below.

NASA Field Centers and Program Offices

Ames Research Center
David Morse
(650) 604-4724
david.r.morse@nasa.gov

Dryden Flight Research Center
Ron Young
(661) 276-3741
ronald.m.young@nasa.gov

Glenn Research Center
Kimberly A. Dalgleish-Miller
(216) 433-8047
kimberly.a.dalgleish@nasa.gov

Goddard Space Flight Center
Nona Cheeks
(301) 286-5810
nona.k.cheeks@nasa.gov

Jet Propulsion Laboratory
Indrani Graczyk
(818) 354-2241
indrani.graczyk@jpl.nasa.gov

Johnson Space Center
John E. James
(281) 483-3809
john.e.james@nasa.gov

Kennedy Space Center
David R. Makufka
(321) 867-6227
david.r.makufka@nasa.gov

Langley Research Center
Michelle Ferebee
(757) 864-5617
michelle.t.ferebee@nasa.gov

Marshall Space Flight Center
Terry L. Taylor
(256) 544-5916
terry.taylor@nasa.gov

Stennis Space Center
Ramona Travis
(228) 688-3832
ramona.e.travis@ssc.nasa.gov

NASA Headquarters

Daniel Lockney,
Technology Transfer Program Executive
(202) 358-2037
daniel.p.lockney@nasa.gov

Small Business Innovation Research (SBIR) & Small Business Technology Transfer (STTR) Programs
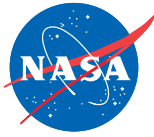Rich Leshner, Program Executive
(202) 358-4920
rleshner@nasa.gov

NASA TECH BRIEFS

NATIONAL AERONAUTICS AND SPACE ADMINISTRATION

Technology Focus: Data Acquisition

iGlobe Interactive Visualization and Analysis of Spatial Data

Ames Research Center, Moffett Field, California

iGlobe is open-source software built on NASA World Wind virtual globe technology. iGlobe provides a growing set of tools for weather science, climate research, and agricultural analysis. Up until now, these types of sophisticated tools have been developed in isolation by national agencies, academic institutions, and research organizations. By providing an open-source solution to analyze and visualize weather, climate, and agricultural data, the scientific and research communities can more readily advance solutions needed to understand better the dynamics of our home planet, Earth.

iGlobe provides a flexible interface for sophisticated analysis and highly interactive visualization of NetCDF (Network Common Data Format) data. NetCDF, the data format typically used for weather and climate data, is large and complex in nature. Even the simple act of accessing NetCDF data is a computation- and data-storage-intensive undertaking. iGlobe is there for the international community to advance collectively solutions that address issues of concern to all.

iGlobe is a 4D virtual globe application using NASA World Wind visualization technology (www.goworldwind.org). iGlobe integrates analysis of climate model outputs and remote sensing observations, combined with demographic and environmental data sets, to understand global and regional phenomena better, and provides impact analysis on a critical national resource, our agricultural industry. iGlobe allows seamless access to remote data repositories, allows users to run sophisticated data analysis algorithms on the server side, and provides accelerated statistical analysis on the client side via a thin client analytic engine able to incorporate server-side processing power.

iGlobe server-side analysis provides support for different data analysis algorithms purposed to identify patterns in spatial-temporal data, i.e., change detection, anomaly detection, clustering, and frequent-pattern analysis. The iGlobe client-side analysis also provides support for statistical operations on selected regions using any number of spatial-temporal data layers and parameters, i.e., spatial mean, median, variance, autocorrelation, etc.

This work was done by Patrick Hogan of Ames Research Center. Further information is contained in a TSP (see page 1). ARC-15166-1A

Broad-Bandwidth FPGA-Based Digital Polyphase Spectrometer

Applications include microwave radiometers, laser heterodyne systems, and radar.

NASA's Jet Propulsion Laboratory, Pasadena, California

With present concern for ecological sustainability ever increasing, it is desirable to model the composition of Earth's upper atmosphere accurately with regards to certain helpful and harmful chemicals, such as greenhouse gases and ozone. The microwave limb sounder (MLS) is an instrument designed to map the global day-to-day concentrations of key atmospheric constituents continuously. One important component in MLS is the spectrometer, which processes the raw data provided by the receivers into frequency-domain information that cannot only be transmitted more efficiently, but also processed directly once received. The present-generation spectrometer is fully analog. The goal is to include a fully digital spectrometer in the next-generation sensor. In a digital spectrometer, incoming analog data must be converted into a digital format, processed through a Fourier transform, and finally accumulated to reduce the impact of input noise. While the final design will be placed on an application specific integrated circuit (ASIC), the building of these chips is prohibitively expensive. To that end, this design was constructed on a field-programmable gate array (FPGA).

A family of state-of-the-art digital Fourier transform spectrometers has been developed, with a combination of high bandwidth and fine resolution. Analog signals consisting of radiation emitted by constituents in planetary atmospheres or galactic sources are down-converted and subsequently digitized by a pair of interleaved analog-to-digital converters (ADCs). This 6-Gsps (gigasample per second) digital representation of the analog signal is then processed through an FPGA-based streaming fast Fourier transform (FFT). Digital spectrometers have many advantages over previously used analog spectrometers, especially in terms of accuracy and resolution, both of which are particularly important for the type of scientific questions to be addressed with next-generation radiometers.

The high-level building blocks (filter and FFT components) were optimized for the Xilinx Virtex 5 FPGA, and for interfacing with one another. The design, from building blocks to complete implementation, was floor-planned in order to make efficient use of the FPGA resources. As more aggressive spectrometer designs were created, designing the hardware to run at a sufficiently high clock rate became progressively more difficult. These issues were mitigated by duplicating hardware and adding (or removing) latency as necessary. The floor-planning of the design was changed dramatically from the original.

The final spectrometer design is an 8192-channel implementation. Designed with additional output capacity, the spectrometer has superior fre-

Measured Channel Frequency Response From 8192 Channel Spectrometer
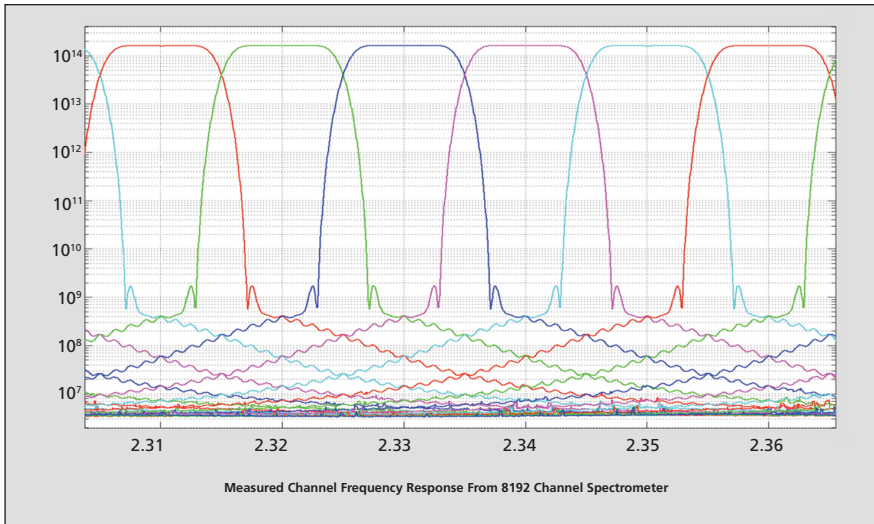
The measured channel frequency response from the 8192-channel **Spectrometer**.

In addition, a further improved spectrometer with double the frequency resolution, a polyphase-FIR filter front end, and substantially reduced noise has been successfully simulated and is presently in the final stages of development. When finished, it will offer a spectrometer developed on Virtex-5 hardware with bandwidth and spectral resolution an order of magnitude greater than the analog spectrometers presently in use.

Plans to make an 8-GHz spectrometer taking advantage of the same technology used for this device are already being made. Finally, efforts are presently being made to interface this design to a compact Nallatech board, which consumes less power and can be more readily used in remote locations and demanding environments.

This work was done by Robert F. Jarnot of Caltech and Ryan M. Monroe of Georgia Tech for NASA's Jet Propulsion Laboratory. Further information is contained in a TSP (see page 1). NPO-48352

quency resolution, dynamic range, and accumulation length when compared to previous versions. An alternate, dual-polarization, 1.5-GHz, 4096-channel spectrometer is available as well. Both designs are capable of accumulating for hours, several orders of magnitude over what is required.

Small Aircraft Data Distribution System

NASA's Jet Propulsion Laboratory, Pasadena, California

The CARVE Small Aircraft Data Distribution System acquires the aircraft location and attitude data that is required by the various programs running on a distributed network. This system distributes the data it acquires to the data acquisition programs for inclusion in their data files.

It uses UDP (User Datagram Protocol) to broadcast data over a LAN (Local Area Network) to any programs that might have a use for the data. The program is easily adaptable to acquire additional data and log that data to disk.

The current version also drives displays using precision pitch and roll information to aid the pilot in maintaining a level-level attitude for radar/radiometer mapping beyond the degree available by flying visually or using a standard gyro-driven attitude indicator.

The software is designed to acquire an array of data to help the mission manager make real-time decisions as to the effectiveness of the flight. This data is displayed for the mission manager and broadcast to the other experiments on the aircraft for inclusion in their data

files. The program also drives real-time precision pitch and roll displays for the pilot and copilot to aid them in maintaining the desired attitude, when required, during data acquisition on mapping lines.

This work was done by Seth L. Chazanoff and Steven J. Dinardo of Caltech for NASA's Jet Propulsion Laboratory. For more information, contact iaoffice@jpl.nasa.gov.

This software is available for commercial licensing. Please contact Daniel Broderick of the California Institute of Technology at danielb@caltech.edu. Refer to NPO-48384.

Earth Science Datacasting v2.0

NASA's Jet Propulsion Laboratory, Pasadena, California

The Datacasting software, which consists of a server and a client, has been developed as part of the Earth Science (ES) Datacasting project. The goal of ES Datacasting is to provide scientists the ability to automatically and continuously download Earth science data that meets a precise, predefined need, and then to instantaneously visualize it on a local computer. This is achieved by applying

the concept of podcasting to deliver science data over the Internet using RSS (Really Simple Syndication) XML feeds. By extending the RSS specification, scientists can filter a feed and only download the files that are required for a particular application (for example, only files that contain information about a particular event, such as a hurricane or flood). The extension also provides the

ability for the client to understand the format of the data and visualize the information locally.

The server part enables a data provider to create and serve basic Datacasting (RSS-based) feeds. The user can subscribe to any number of feeds, view the information related to each item contained within a feed (including browse pre-made images),

manually download files associated with items, and place these files in a local store.

The client-server architecture enables users to:
- Subscribe and interpret multiple Data-casting feeds (same look and feel as a typical mail client),
- Maintain a list of all items within each feed,

- Enable filtering on the lists based on different metadata attributes contained within the feed (list will reference only data files of interest),
- Visualize the reference data and associated metadata,
- Download files referenced within the list, and
- Automatically download files as new items become available.

❯ Algorithm for Compressing Time-Series Data
This algorithm is generally applicable to many types of data.

Goddard Space Flight Center, Greenbelt, Maryland

An algorithm based on Chebyshev polynomials effects lossy compression of time-series data or other one-dimensional data streams (e.g., spectral data) that are arranged in blocks for sequential transmission. The algorithm was developed for use in transmitting data from spacecraft scientific instruments to Earth stations. In spite of its lossy nature, the algorithm preserves the information needed for scientific analysis. The algorithm is computationally simple, yet compresses data streams by factors much greater than two. The algorithm is not restricted to spacecraft or scientific uses: it is applicable to time-series data in general. The algorithm can also be applied to general multidimensional data that have been converted to time-series data, a typical example being image data acquired by raster scanning. However, unlike most prior image-data-compression algorithms, this algorithm neither depends on nor exploits the two-dimensional spatial correlations that are generally present in images.

In order to understand the essence of this compression algorithm, it is necessary to understand that the net effect of this algorithm and the associated decompression algorithm is to approximate the original stream of data as a sequence of finite series of Chebyshev polynomials. For the purpose of this algorithm, a block of data or interval of time for which a Chebyshev polynomial series is fitted to the original data is denoted a fitting interval. Chebyshev approximation has two properties that make it particularly effective for compressing serial data streams with minimal loss of scientific information: The errors associated with a Chebyshev approximation are nearly uniformly distributed over the fitting interval (this is

Chebyshev Transforms are calculated in this algorithm, which effects lossy compression of data. Parameters of the algorithm can be adjusted to balance accuracy versus degree of compression.

known in the art as the "equal error property"); and the maximum deviations of the fitted Chebyshev polynomial from the original data have the smallest possible values (this is known in the art as the "min-max property").

The algorithm performs the same sequence of calculations on each successive data block (see figure). For each block, the first step is a calculation of a Chebyshev transform; that is, a matrix of coefficients of a Chebyshev series. This involves calculation of linear combinations of data samples with the applicable Chebyshev coefficients. The Chebyshev coefficients are fixed and known, making it possible to reduce the computational burden by computing them in advance, storing them in lookup tables, and retrieving them from the lookup tables as needed. In the next step, the matrix of coefficients is thresholded: only those coefficients larger than a threshold specified by the user are retained. The retained coefficients are then quantized to reduce their representations to no more than a number of bits specified by the user.

Next, there is generated a bit-control word, which is to be used during the subsequent decompression process to indicate the locations for insertion of the quantized retained coefficients and for insertion of place holders (zeroes) at locations of coefficients that are not retained. The bit-control word is then encoded by a lossless compression technique; this step can significantly increase the overall compression ratio without introducing additional loss. If there are more data blocks to be processed, then the process as described thus far is repeated for the next block. If there are no more blocks to be processed, the compressed data and their control words are transmitted.
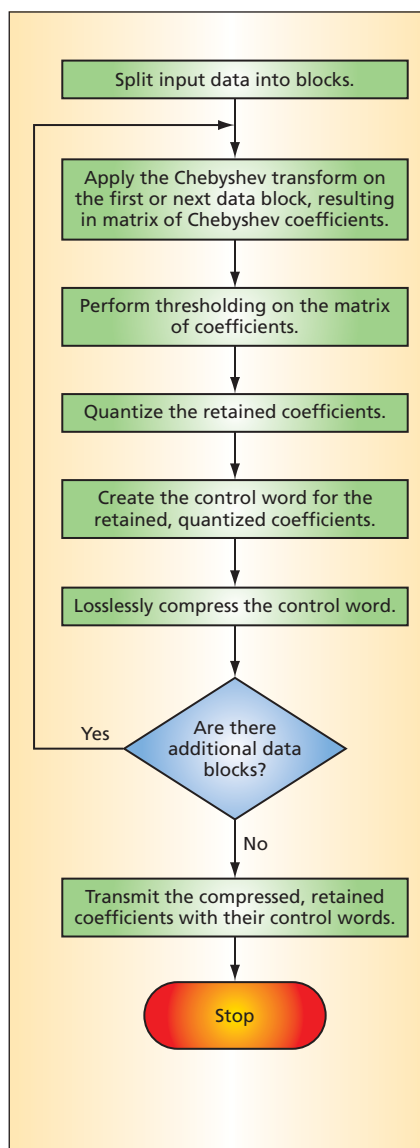
The results obtained by use of the algorithm depend partly on three parameters: the block size (the number of data samples in a block), the aforementioned threshold value, and the aforementioned number of quantization bits. By adjusting the values of these parameters for different types of data, one can obtain usefully large compression ratios with minimal errors. Higher threshold values always result in greater compression ratios at the expense of quality of reconstructed signals. Increasing numbers of quantization bits generally reduces compression ratios but yields reconstructed signals of higher quality. Increasing block sizes yields more-varied results; in general, larger compression ratios are associated with larger blocks because fewer block maxima and minima are stored.

This work was done by S. Edward Hawkins III and Edward Hugo Darlington of Johns Hopkins University Applied Physics Laboratory for Goddard Space Flight Center. For further information, contact the Goddard Innovative Partnerships Office at (301) 286-5810. GSC-14820-1

❯ Onboard Science and Applications Algorithm for Hyperspectral Data Reduction

NASA's Jet Propulsion Laboratory, Pasadena, California

An onboard processing mission concept is under development for a possible Direct Broadcast capability for the HyspIRI mission, a Hyperspectral remote sensing mission under consideration for launch in the next decade. The concept would intelligently spectrally and spatially subsample the data as well as generate science products onboard to enable return of key rapid response science and applications information despite limited downlink bandwidth. This rapid data delivery concept focuses on wildfires and volcanoes as primary applications, but also has applications to vegetation, coastal flooding, dust, and snow/ice applications.

Operationally, the HyspIRI team would define a set of spatial regions of interest where specific algorithms would be executed. For example, known coastal areas would have certain products or bands downlinked, ocean areas might have other bands downlinked, and during fire seasons other areas would be processed for active fire detections. Ground operations would automatically generate the mission plans specifying the highest priority tasks executable within onboard computation, setup, and data downlink constraints.

The spectral bands of the TIR (thermal infrared) instrument can accurately detect the thermal signature of fires and send down alerts, as well as the thermal and VSWIR (visible to short-wave infrared) data corresponding to the active fires. Active volcanism also produces a distinctive thermal signature that can be detected onboard to enable spatial subsampling. Onboard algorithms and ground-based algorithms suitable for onboard deployment are mature. On HyspIRI, the algorithm would perform a table-driven temperature inversion from several spectral TIR bands, and then trigger downlink of the entire spectrum for each of the hot pixels identified.

Ocean and coastal applications include sea surface temperature (using a small spectral subset of TIR data, but requiring considerable ancillary data), and ocean color applications to track biological activity such as harmful algal blooms. Measuring surface water extent to track flooding is another rapid response product leveraging VSWIR spectral information.

This work was done by Steve A. Chien, Ashley G. Davies, and Dorothy Silverman of Caltech for NASA's Jet Propulsion Laboratory, and Daniel Mandl of Goddard Space Flight Center. For more information, contact iaoffice@jpl.nasa.gov. NPO-47471

❯ Sampling Technique for Robust Odorant Detection Based on MIT RealNose Data

NASA's Jet Propulsion Laboratory, Pasadena, California

This technique enhances the detection capability of the autonomous RealNose system from MIT to detect odorants and their concentrations in noisy and transient environments. The low-cost, portable system with low power consumption will operate at high speed and is suited for unmanned and remotely operated long-life applications.

A deterministic mathematical model was developed to detect odorants and calculate their concentration in noisy environments. Real data from MIT's NanoNose was examined, from which a signal conditioning technique was proposed to enable robust odorant detection for the RealNose system. Its sensitivity can reach to sub-part-per-billion (sub-ppb).

A Space Invariant Independent Component Analysis (SPICA) algorithm was developed to deal with non-linear mixing that is an over-complete case, and it is used as a preprocessing step to recover the original odorant sources for detection. This approach, combined with the Cascade Error Projection (CEP) Neural Network algorithm, was used to perform odorant identification.

Signal conditioning is used to identify potential processing windows to enable robust detection for autonomous systems. So far, the software has been developed and evaluated with current data sets provided by the MIT team. However, continuous data streams are made available where even the occurrence of a new odorant is unannounced and needs to be noticed by the system autonomously before its unambiguous detection. The challenge for the software is to be able to separate the potential valid signal from the odorant and from the noisy transition region when the odorant is just introduced.

This work was done by Tuan A. Duong of Caltech for NASA's Jet Propulsion Laboratory. For more information, contact iaoffice@jpl.nasa.gov. NPO-47488

Security Data Warehouse Application

Lyndon B. Johnson Space Center, Houston, Texas

The Security Data Warehouse (SDW) is used to aggregate and correlate all JSC IT security data. This includes IT asset inventory such as operating systems and patch levels, users, user logins, remote access dial-in and VPN, and vulnerability tracking and reporting. The correlation of this data allows for an integrated understanding of current security issues and systems by providing this data in a format that associates it to an individual host. The cornerstone of the SDW is its unique host-mapping algorithm that has undergone extensive field tests, and provides a high degree of accuracy.

The algorithm comprises two parts. The first part employs fuzzy logic to derive a best-guess host assignment using incomplete sensor data. The second part is logic to identify and correct errors in the database, based on subsequent, more complete data. Host records are automatically split or merged, as appropriate.

The process had to be refined and thoroughly tested before the SDW deployment was feasible. Complexity was increased by adding the dimension of time. The SDW correlates all data with its relationship to time. This lends support to forensic investigations, audits, and overall situational awareness.

Another important feature of the SDW architecture is that all of the underlying complexities of the data model and host-mapping algorithm are encapsulated in an easy-to-use and understandable Perl language Application Programming Interface (API). This allows the SDW to be quickly augmented with additional sensors using minimal coding and testing. It also supports rapid generation of ad hoc reports and integration with other information systems.

This work was done by Lynn R. Vernon, Robert Hennan, Chris Ortiz, and Steve Gonzalez of Johnson Space Center, and John Roane of MEI Technologies. For further information, contact the JSC Innovation Partnerships Office at (281) 483-3809.

In accordance with Public Law 96-517, the contractor has elected to retain title to this invention. Inquiries concerning rights for its commercial use should be addressed to:

MEI Technologies
2525 Bay Area Blvd., Suite 300
Houston, TX 77058
Phone No.: (281) 283-6200
E-mail: meiinfo@meitechnic.com
Refer to MSC-24148-1, volume and number of this NASA Tech Briefs *issue, and the page number.*

Integrated Laser Characterization, Data Acquisition, and Command and Control Test System

Goddard Space Flight Center, Greenbelt, Maryland

Satellite-based laser technology has been developed for topographical measurements of the Earth and of other planets. Lasers for such missions must be highly efficient and stable over long periods in the temperature variations of orbit. In this innovation, LabVIEW is used on an Apple Macintosh to acquire and analyze images of the laser beam as it exits the laser cavity to evaluate the laser's performance over time, and to monitor and control the environmental conditions under which the laser is tested. One computer attached to multiple cameras and instruments running LabVIEW-based software replaces a conglomeration of computers and software packages, saving hours in maintenance and data analysis, and making very long-term tests possible.

This all-in-one system was written primarily using LabVIEW for Mac OS X, which allows the combining of data from multiple RS-232, USB, and Ethernet instruments for comprehensive laser analysis and control. The system acquires data from CCDs (charge coupled devices), power meters, thermistors, and oscilloscopes over a controllable period of time. This data is saved to an html file that can be accessed later from a variety of data analysis programs. Also, through the LabVIEW interface, engineers can easily control laser input parameters such as current, pulse width, chiller temperature, and repetition rates. All of these parameters can be adapted and cycled over a period of time.

This work was done by Paul Stysley and Barry Coyle of Goddard Space Flight Center, and Eric Lyness of Mink Hollow Systems, Inc. Further information is contained in a TSP (see page 1). GSC-16298-1

Electronics/Computers

Radiation-Hard SpaceWire/Gigabit Ethernet-Compatible Transponder

Transponder features low power and low fabrication cost.

Goddard Space Flight Center, Greenbelt, Maryland

A radiation-hard transponder was developed utilizing submicron/nano-technology from IBM. The device consumes low power and has a low fabrication cost. This device utilizes a Plug-and-Play concept, and can be integrated into intra-satellite networks, supporting SpaceWire and Gigabit Ethernet I/O. A space-qualified, 100-pin package also was developed, allowing space-qualified (class K) transponders to be delivered within a six-month time frame.

The novel, optical, radiation-tolerant transponder was implemented as a standalone board, containing the transponder ASIC (application specific integrated circuit) and optical module, with an FPGA (field-programmable gate array) friendly parallel interface. It features improved radiation tolerance; high-data-rate, low-power consumption; and advanced functionality. The transponder utilizes a patented current-mode logic library of radiation-hardened-by-architecture cells. The transpon-

der was developed, fabricated, and rad-hard tested up to 1 MRad. It was fabricated using 90-nm CMOS (complementary metal oxide semiconductor) 9 SF process from IBM, and incorporates full BIT circuitry, allowing a loop back test.

The low-speed parallel LVCMOS (low-voltage complementary metal oxide semiconductor) bus is compatible with Actel FPGA. The output LVDS (low-voltage differential signaling) interface operates up to 1.5 Gb/s. Built-in CDR (clock-data recovery) circuitry provides robust synchronization and incorporates two alarm signals such as synch loss and signal loss. The ultra-linear peak detector scheme allows on-line control of the amplitude of the input signal. Power consumption is less than 300 mW.

The developed transponder with a 1.25 Gb/s serial data rate incorporates a 10-to-1 serializer with an internal clock multiplication unit and a 10-1 deserializer with internal clock and data recovery block, which can operate with 8B10B

encoded signals. Three loop-back test modes are provided to facilitate the built-in-test functionality. The design is based on a proprietary library of differential current switching logic cells implemented in the standard 90-nm CMOS 9SF technology from IBM. The proprietary low-power LVDS physical interface is fully compatible with the SpaceWire standard, and can be directly connected to the SFP MSA (small form factor pluggable Multiple Source Agreement) optical transponder. The low-speed parallel interfaces are fully compatible with the standard 1.8 V CMOS input/output devices. The utilized proprietary annular CMOS layout structures provide TID tolerance above 1.2 MRad. The complete chip consumes less than 150 mW of power from a single 1.8-V positive supply source.

This work was done by Vladimir Katzman of Adsantec for Goddard Space Flight Center. Further information is contained in a TSP (see page 1). GSC-16038-1

Hardware Implementation of Lossless Adaptive Compression of Data From a Hyperspectral Imager

Implementation uses a new version of the algorithm that targets pushbroom-type imagers in order to be suitable for use on satellites.

NASA's Jet Propulsion Laboratory, Pasadena, California

Efficient onboard data compression can reduce the data volume from hyperspectral imagers on NASA and DoD spacecraft in order to return as much imagery as possible through constrained downlink channels. Lossless compression is important for signature extraction, object recognition, and feature classification capabilities. To provide onboard data compression, a hardware implementation of a lossless hyperspectral compression algorithm was developed using a field programmable gate array (FPGA). The underlying algorithm is the Fast Lossless (FL) com-

pression algorithm reported in "Fast Lossless Compression of Multispectral-Image Data" (NPO-42517), *NASA Tech Briefs*, Vol. 30, No. 8 (August 2006), p. 26 with the modification reported in "Lossless, Multi-Spectral Data Comressor for Improved Compression for Pushbroom-Type Instruments" (NPO-45473), *NASA Tech Briefs*, Vol. 32, No. 7 (July 2008) p. 63, which provides improved compression performance for data from pushbroom-type imagers. An FPGA implementation of the unmodified FL algorithm was previously developed and reported in "Fast and Adaptive Lossless

Onboard Hyperspectral Data Compression System" (NPO-46867), *NASA Tech Briefs*, Vol. 36, No. 5 (May 2012) p. 42. The essence of the FL algorithm is adaptive linear predictive compression using the sign algorithm for filter adaption. The FL compressor achieves a combination of low complexity and compression effectiveness that exceeds that of state-of-the-art techniques currently in use. The modification changes the predictor structure to tolerate differences in sensitivity of different detector elements, as occurs in pushbroom-type imagers, which are suitable for spacecraft use.

The FPGA implementation offers a low-cost, flexible solution compared to traditional ASIC (application specific integrated circuit) and can be integrated as an intellectual property (IP) for part of, e.g., a design that manages the instrument interface. The FPGA implementation was benchmarked on the Xilinx Virtex IV LX25 device, and ported to a Xilinx prototype board. The current implementation has a critical path of 29.5 ns, which dictated a clock speed of 33 MHz. The critical path delay is end-to-end measurement between the uncompressed input data and the output compression data stream. The implementation compresses one sample every clock cycle, which results in a speed of 33 Msample/s. The implementation has a rather low device use of the Xilinx Virtex IV LX25, making the total power consumption of the implementation about 1.27 W.

This work was done by Didier Keymeulen, Nazeeh I. Aranki, and Matthew A. Klimesh of Caltech, and Alireza Bakhshi of B&A Engineering for NASA's Jet Propulsion Laboratory. For more information, contact iaoffice@jpl.nasa.gov. NPO-47103

High-Voltage, Low-Power BNC Feedthrough Terminator

John F. Kennedy Space Center, Florida

This innovation is a high-voltage, low-power BNC (Bayonet Neill–Concelman) feedthrough that enables the user to terminate an instrumentation cable properly while connected to a high voltage, without the use of a voltage divider. This feedthrough is low power, which will not load the source, and will properly terminate the instrumentation cable to the instrumentation, even if the cable impedance is not constant.

The Space Shuttle Program had a requirement to measure voltage transients on the orbiter bus through the Ground Lightning Measurement System (GLMS). This measurement has a bandwidth requirement of 1 MHz. The GLMS voltage measurement is connected to the orbiter through a DC panel. The DC panel is connected to the bus through a nonuniform cable that is approximately 75 ft (≈23 m) long. A 15-ft (≈5-m), 50-ohm triaxial cable is connected between the DC panel and the digitizer. Based on calculations and simulations, cable resonances and reflections due to mismatched impedances of the cable connecting the orbiter bus and the digitizer causes the output not to reflect accurately what is on the bus. A voltage divider at the DC panel, and terminating the 50-ohm cable properly, would eliminate this issue. Due to implementation issues, an alternative design was needed to terminate the cable properly without the use of a voltage divider.

Analysis shows how the cable resonances and reflections due to the mismatched impedances of the cable connecting the orbiter bus and the digitizer causes the output not to reflect accurately what is on the bus. After simulating a dampening circuit located at the digitizer, simulations were performed to show how the cable resonances were dampened and the accuracy was improved significantly. Test cables built to verify simulations were accurate. Since the dampening circuit is low power, it can be packaged in a BNC feedthrough.

This work was done by Douglas (Doug) Bearden of Kennedy Space Center. Further information is contained in a TSP (see page 1). KSC-13560

SpaceCube Mini

A unit that is being designed will be a very compact and low-power system.

Goddard Space Flight Center, Greenbelt, Maryland

This version of the SpaceCube will be a full-fledged, onboard space processing system capable of 2500+ MIPS, and featuring a number of plug-and-play gigabit and standard interfaces, all in a condensed 3×3×3 form factor [<10 watts and < 3 lb (≈1.4 kg)]. The main processing engine is the Xilinx SIRF radiation-hardened-by-design Virtex-5 FX-130T field-programmable gate array (FPGA).

Even as the SpaceCube 2.0 version (currently under test) is being targeted as the platform of choice for a number of the upcoming Earth Science Decadal Survey missions, GSFC has been contacted by customers who wish to see a system that incorporates key features of the version 2.0 architecture in an even smaller form factor. In order to fulfill that need, the SpaceCube Mini is being designed, and will be a very compact and low-power system. A similar flight system with this combination of small size, low power, low cost, adaptability, and extremely high processing power does not otherwise exist, and the SpaceCube Mini will be of tremendous benefit to GSFC and its partners.

The SpaceCube Mini will utilize space-grade components. The primary processing engine of the Mini is the Xilinx Virtex-5 SIRF FX-130T radiation-hardened-by-design FPGA for critical flight applications in high-radiation environments. The Mini can also be equipped with a commercial Xilinx Virtex-5 FPGA with integrated PowerPCs for a low-cost, high-power computing platform for use in the relatively radia- tion-benign LEOs (low-Earth orbits). In either case, this version of the Space-Cube will weigh less than 3 pounds (≈1.4 kg), conform to the CubeSat form-factor (10×10×10 cm), and will be low power (<10 watts for typical applications). The SpaceCube Mini will have a radiation-hardened Aeroflex FPGA for configuring and scrubbing the Xilinx FPGA by utilizing the onboard FLASH memory to store the configuration files. The FLASH memory will also be used for storing algorithm and application code for the PowerPCs and the Xilinx FPGA. In addition, it will feature high-speed DDR SDRAM (double data rate synchronous dynamic random-access memory) to store the instructions and data of active applications. This version will also feature SATA-II and Gigabit

Ethernet interfaces. Furthermore, there will also be general-purpose, multi-gigabit interfaces. In addition, the system will have dozens of transceivers that can support LVDS (low-voltage differential signaling), RS-422, or SpaceWire. The SpaceCube Mini includes an I/O card that can be customized to meet the needs of each mission. This version of the SpaceCube will be designed so that multiple Minis can be networked to-

gether using SpaceWire, Ethernet, or even a custom protocol.

Scalability can be provided by networking multiple SpaceCube Minis together. Rigid-Flex technology is being targeted for the construction of the SpaceCube Mini, which will make the extremely compact and low-weight design feasible. The SpaceCube Mini is designed to fit in the compact CubeSat form factor, thus allowing deployment in

a new class of missions that the previous SpaceCube versions were not suited for. At the time of this reporting, engineering units should be available in the summer 2012.

This work was done by Michael Lin, David Petrick, Alessandro Geist, and Thomas Flatley of Goddard Space Flight Center. Further information is contained in a TSP (see page 1). GSC-16223-1

Dichroic Filter for Separating W-Band and Ka-Band

NASA's Jet Propulsion Laboratory, Pasadena, California

The proposed Aerosol/Cloud/Ecosystems (ACEs) mission development would advance cloud profiling radar from that used in CloudSat by adding a 35-GHz (Ka-band) channel to the 94-GHz (W-band) channel used in CloudSat. In order to illuminate a single antenna, and use CloudSat-like quasi-optical transmission lines, a spatial diplexer is needed to add the Ka-band channel.

A dichroic filter separates Ka-band from W-band by employing advances in electrical discharge machining (EDM) and mode-matching analysis techniques developed and validated for designing dichroics for the Deep Space Network (DSN), to develop a preliminary design that both met the requirements of frequency separation and mechanical strength.

First, a mechanical prototype was built using an approximately 102-micron-diameter EDM process, and tolerances of the hole dimensions, wall thickness, radius, and dichroic filter thickness measured. The prototype validated the manufacturing needed to design a dichroic filter for a higher-frequency usage than previously used in the DSN. The initial design was based on a Ka-band design, but thicker walls are required for mechanical rigidity than one obtains by simply scaling the Ka-band dichroic filter. The resulting trade of hole dimensions for mechanical rigidity (wall thickness) required electrical redesign of the hole dimensions. Updates to existing codes in the linear solver decreased the analysis time using mode-matching, en-

abling the electrical design to be realized quickly.

This work is applicable to missions and instruments that seek to extend W-band cloud profiling measurements to other frequencies. By demonstrating a dichroic filter that passes W-band, but reflects a lower frequency, this opens up the development of instruments that both compare to and enhance CloudSat.

This work was done by Larry W. Epp, Stephen L. Durden, Vahraz Jamnejad, Ezra M. Long, John B. Sosnowski, Raymond J. Higuera, and Jacqueline C. Chen of Caltech for NASA's Jet Propulsion Laboratory. Further information is contained in a TSP (see page 1). NPO-48174

Software

Active Mirror Predictive and Requirements Verification Software (AMP-ReVS)

This software is designed to predict large active mirror performance at various stages in the fabrication lifecycle of the mirror. It was developed for 1-meter class powered mirrors for astronomical purposes, but is extensible to other geometries. The package accepts finite element model (FEM) inputs and laboratory measured data for large optical-quality mirrors with active figure control. It computes phenomenological contributions to the surface figure error using several built-in optimization techniques. These phenomena include stresses induced in the mirror by the manufacturing process and the support structure, the test procedure, high spatial frequency errors introduced by the polishing process, and other process-dependent deleterious effects due to light-weighting of the mirror. Then, depending on the maturity of the mirror, it either predicts the best surface figure error that the mirror will attain, or it verifies that the requirements for the error sources have been met once the best surface figure error has been measured.

The unique feature of this software is that it ties together physical phenomenology with wavefront sensing and control techniques and various optimization methods including convex optimization, Kalman filtering, and quadratic programming to both generate predictive models and to do requirements verification. This software combines three distinct disciplines: wavefront control, predictive models based on FEM, and requirements verification using measured data in a robust, reusable code that is applicable to any large optics for ground and space telescopes.

The software also includes state-of-the-art wavefront control algorithms that allow closed-loop performance to be computed. It allows for quantitative trade studies to be performed for optical systems engineering, including computing the best surface figure error under various testing and operating conditions. After the mirror manufacturing process and testing have been completed, the software package can be used to verify that the underlying requirements have been met.

Navigation/Prop Software Suite

Navigation (Nav)/Prop software is used to support shuttle mission analysis, production, and some operations tasks. The Nav/Prop suite containing configuration items (CIs) resides on IPS/Linux workstations. It features lifecycle documents, and data files used for shuttle navigation and propellant analysis for all flight segments. This suite also includes trajectory server, archive server, and RAT software residing on MCC/Linux workstations.

Navigation/Prop represents tool versions established during or after IPS Equipment Rehost-3 or after the MCC Rehost.

Personal Computer Transport Analysis Program

The Personal Computer Transport Analysis Program (PCTAP) is C++ software used for analysis of thermal fluid systems. The program predicts thermal fluid system and component transients. The output consists of temperatures, flow rates, pressures, delta pressures, tank quantities, and gas quantities in the air, along with air scrubbing component performance.

PCTAP's solution process assumes that the tubes in the system are well insulated so that only the heat transfer between fluid and tube wall and between adjacent tubes is modeled. The system described in the model file is broken down into its individual components; i.e., tubes, cold plates, heat exchangers, etc. A solution vector is built from the components and a flow is then simulated with fluid being transferred from one component to the next. The solution vector of components in the model file is built at the initiation of the run. This solution vector is simply a list of components in the order of their inlet dependency on other components. The component parameters are updated in the order in which they appear in the list at every time step. Once the solution vectors have been determined, PCTAP cycles through the components in the solution vector, executing their outlet function for each time-step increment.

Pressure Ratio to Thermal Environments

A pressure ratio to thermal environments (PRatTlE.pl) program is a Perl language code that estimates heating at requested body point locations by scaling the heating at a reference location times a pressure ratio factor. The pressure ratio factor is the ratio of the local pressure at the reference point and the requested point from CFD (computational fluid dynamics) solutions.

This innovation provides pressure ratio-based thermal environments in an automated and traceable method. Previously, the pressure ratio methodology was implemented via a Microsoft Excel spreadsheet and macro scripts. PRatTlE is able to calculate heating environments for 150 body points in less than two minutes.

PRatTlE is coded in Perl programming language, is command-line-driven, and has been successfully executed on both the HP and Linux platforms. It supports multiple concurrent runs. PRatTlE

contains error trapping and input file format verification, which allows clear visibility into the input data structure and intermediate calculations

This work was done by Pedro Lopez and Winston Wang of The Boeing Co. for Johnson Space Center. For further information, contact the JSC Innovation Partnerships Office at (281) 483-3809. MSC-24963-1

Probabilistic Fatigue Damage Program (FATIG)

FATIG computes fatigue damage/fatigue life using the stress rms (root mean square) value, the total number of cycles, and S–N curve parameters. The damage is computed by the following methods: (a) traditional method using Miner's rule with stress cycles determined from a Rayleigh distribution up to 3*sigma; and (b) classical fatigue damage formula involving the Gamma function, which is derived from the integral version of Miner's rule. The integration is carried out over all stress amplitudes.

This software solves the problem of probabilistic fatigue damage using the integral form of the Palmgren-Miner rule. The software computes fatigue life using an approach involving all stress amplitudes, up to N*sigma, as specified by the user.

It can be used in the design of structural components subjected to random dynamic loading, or by any stress analyst with minimal training for fatigue life estimates of structural components.

This work was done by Constantine Michalopoulos of The Boeing Co. for Johnson Space Center. For further information, contact the JSC Innovation Partnerships Office at (281) 483-3809. MSC-24975-1

ASCENT Program

The ASCENT program solves the three-dimensional motion and attendant structural loading on a flexible vehicle incorporating, optionally, an active analog thrust control system, aerodynamic effects, and staging of multiple bodies.

ASCENT solves the technical problems of loads, accelerations, and displacements of a flexible vehicle; staging of the upper stage from the lower stage; effects of thrust oscillations on the vehicle; a payload's relative motion; the effect of fluid sloshing on vehicle; and the effect of winds and gusts on the vehicle (on the ground or aloft) in a continuous analysis.

The ATTACH ASCENT Loads program reads output from the ASCENT flexible body loads program, and calculates the approximate load indicators for the time interval under consideration. It calculates the load indicator values from pre-launch to the end of the first stage.

This work was done by Richard Brown, Gary Collier, Richard Heckenlaible, Edward Dougherty, James Dolenz, and Iain Ross of The Boeing Company for Johnson Space Center. For further information, contact the JSC Innovation Partnerships Office at (281) 483-3809. MSC-24978-1/9-1

JPL Genesis and Rapid Intensification Processes (GRIP) Portal

Satellite observations can play a very important role in airborne field campaigns, since they provide a comprehensive description of the environment that is essential for the experiment design, flight planning, and post-experiment scientific data analysis. In the past, it has been difficult to fully utilize data from multiple NASA satellites due to the large data volume, the complexity of accessing NASA's data in near-real-time (NRT), as well as the lack of software tools to interact with multi-sensor information.

The JPL GRIP Portal is a Web portal that serves a comprehensive set of NRT observation data sets from NASA and NOAA satellites describing the atmospheric and oceanic environments related to the genesis and intensification of the tropical storms in the North Atlantic Ocean. Together with the model forecast data from four major global atmospheric models, this portal provides a useful tool for the scientists and forecasters in planning and monitoring the NASA GRIP field campaign during the 2010 Atlantic Ocean hurricane season.

This portal uses the Google Earth plug-in to visualize various types of data sets, such as 2D maps, wind vectors, streamlines, 3D data sets presented at series of vertical cross-sections or pointwise vertical profiles, and hurricane best tracks and forecast tracks. Additionally, it allows users to overlap multiple data sets, change the opacity of each image layer, generate animations on the fly with selected data sets, and compare the observation data with the model forecast using two independent calendars. The portal also provides the capability to identify the geographic location of any point of interest.

In addition to supporting the airborne mission planning, the NRT data and portal will serve as a very rich source of information during the post-field campaign analysis stage of the airborne experiment. By including a diverse set of satellite observations and model forecasts, it provides a good spatial and temporal context for the high-resolution, but limited in space and time, airborne observations.

This work was done by Brian W. Knosp, P. Peggy Li, Quoc A. Vu, Francis J. Turk, Tsae-Pyng J. Shen, Svetla M. Hristova-Veleva, Stephen J. Licata, and William L. Poulsen of Caltech for NASA's Jet Propulsion Laboratory. For more information, contact iaoffice@jpl.nasa.gov.

This software is available for commercial licensing. Please contact Daniel Broderick of the California Institute of Technology at danielb@caltech.edu. Refer to NPO-47787.

Data::Downloader

Downloading and organizing large amounts of files is challenging, and often done using ad hoc methods. This software is capable of downloading and organizing files as an OpenSearch client. It can subscribe to RSS (Really Simple Syndication) feeds and Atom feeds containing arbitrary metadata, and maintains a local content addressable data store. It uses existing standards for obtaining the files, and uses efficient techniques for storing the files. Novel features include symbolic links to maintain a sane directory structure, checksums for validating file integrity during transfer and storage, and flexible use of server-provided metadata.

This work was done by Brian Duggan of Adnet Systems and Curt Tilmes of NASA for Goddard Space Flight Center. For further information, contact the Goddard Innovative Partnerships Office at (301) 286-5810. GSC-16203-1.

Fault Tolerance Middleware for a Multi-Core System

Fault Tolerance Middleware (FTM) provides a framework to run on a dedicated core of a multi-core system and handles detection of single-event upsets (SEUs), and the responses to those SEUs, occurring in an application running on multiple cores of the processor. This software was written expressly for a multi-core system and can support different kinds of fault strategies, such as introspection, algorithm-based fault tolerance (ABFT), and triple modular redundancy (TMR). It focuses on providing fault tolerance for the application code, and represents the first step in a plan to eventually include fault tolerance in message passing and the FTM itself.

In the multi-core system, the FTM resides on a single, dedicated core, separate from the cores used by the application. This is done in order to isolate the FTM from application faults and to allow it to swap out any application core for a substitute. The structure of the FTM consists of an interface to a fault tolerant strategy module, a responder module, a fault manager module, an error factory, and an error mapper that determines the severity of the error.

In the present reference implementation, the only fault tolerant strategy implemented is introspection. The introspection code waits for an application node to send an error notification to it. It then uses the error factory to create an error object, and at this time, a severity level is assigned to the error. The introspection code uses its built-in knowledge base to generate a recommended response to the error. Responses might include ignoring the error, logging it, rolling back the application to a previously saved checkpoint, swapping in a new node to replace a bad one, or restarting the application. The original error and recommended response are passed to the top-level fault manager module, which invokes the response. The responder module also notifies the introspection module of the generated response. This provides additional information to the introspection module that it can use in generating its next response. For example, if the responder triggers an application rollback and errors are still occurring, the introspection module may decide to recommend an application restart.

This work was done by Raphael R. Some, Paul L. Springer, Hans P. Zima, Mark James, and David A. Wagner of Caltech for NASA's Jet Propulsion Laboratory. For more information, contact tiaoffice@jpl.nasa.gov.

This software is available for commercial licensing. Please contact Daniel Broderick of the California Institute of Technology at danielb@caltech.edu. Refer to NPO-47806.

DspaceOgreTerrain 3D Terrain Visualization Tool

DspaceOgreTerrain is an extension to the DspaceOgre 3D visualization tool that supports real-time visualization of various terrain types, including digital elevation maps, planets, and meshes. DspaceOgreTerrain supports creating 3D representations of terrains and placing them in a scene graph. The 3D representations allow for a continuous level of detail, GPU-based rendering, and overlaying graphics like wheel tracks and shadows. It supports reading data from the SimScape terrain-modeling library.

DspaceOgreTerrain solves the problem of displaying the results of simulations that involve very large terrains. In the past, it has been used to visualize simulations of vehicle traverses on Lunar and Martian terrains. These terrains were made up of billions of vertices and would not have been renderable in real-time without using a continuous level of detail rendering technique.

This work was done by Steven Myint, Abhinandan Jain, and Marc I. Pomerantz of Caltech for NASA's Jet Propulsion Laboratory. Further information is contained in a TSP (see page 1).

This software is available for commercial licensing. Please contact Daniel Broderick of the California Institute of Technology at danielb@caltech.edu. Refer to NPO-47976.

Trick Simulation Environment 07

The Trick Simulation Environment is a generic simulation toolkit used for constructing and running simulations. This release includes a Monte Carlo analysis simulation framework and a data analysis package. It produces all auto documentation in XML. Also, the software is capable of inserting a malfunction at any point during the simulation. Trick 07 adds variable server output options and error messaging and is capable of using and manipulating wide characters for international support. Wide character strings are available as a fundamental type for variables processed by Trick.

A Trick Monte Carlo simulation uses a statistically generated, or predetermined, set of inputs to iteratively drive the simulation. Also, there is a framework in place for optimization and solution finding where developers may iteratively modify the inputs per run based on some analysis of the outputs. The data analysis package is capable of reading data from external simulation packages such as MATLAB and Octave, as well as the common comma-separated values (CSV) format used by Excel, without the use of external converters. The file formats for MATLAB and Octave were obtained from their documentation sets, and Trick maintains generic file readers for each format.

XML tags store the fields in the Trick header comments. For header files, XML tags for structures and enumerations, and the members within are stored in the auto documentation. For source code files, XML tags for each function and the calling arguments are stored in the auto documentation. When a simulation is built, a top level XML file, which includes all of the header and source code XML auto documentation files, is created in the simulation directory. Trick 07 provides an XML to TeX converter. The converter reads in header and source code XML documentation files and converts the data to TeX labels and tables suitable for inclusion in TeX documents.

A malfunction insertion capability allows users to override the value of any simulation variable, or call a malfunction job, at any time during the simulation. Users may specify conditions, use the return value of a malfunction trigger job, or manually activate a malfunction. The malfunction action may consist of executing a block of input file statements in an action block, setting simulation variable values, call a malfunction job, or turn on/off simulation jobs.

The variable server output options and error messaging capabilities allow the variable server to return data in a tab delimited ASCII format, or in a record-based binary format. The binary record includes information about the type and size of a variable not present in the ASCII format. The binary option is capable of transmitting full C/C++ structures with one request. With this option, error messaging is returnable to client applications. In this software, the variable server may also return time synchronous data, which is gathered and sent at the end of the simulation frame to guarantee data consistency. Also, the Trick 07 variable server is capable of delivering the simulation data to multiple clients using multicast sockets. This allows multiple machines to receive the same data without increasing the computational load on the simulation.

In addition to Linux and MacOSX, Trick 07 now supports three real-time operating systems: QNX, LynxOS, and RedHawk Linux. Each RTOS has unique system calls accessing real-time features such as setting process priorities, processor assignment, and accessing the real-time clock. Trick uses the unique real-time features of each OS.

This work was done by Alexander S. Lin of Johnson Space Center and John M. Penn, Dan A. Strauss, and Keith Vetter of L-3 Communications Corporation. Further informa-

tion is contained in a TSP (see page 1). MSC-24492-1

⊘ Geometric Reasoning for Automated Planning

An important aspect of mission planning for NASA's operation of the International Space Station is the allocation and management of space for supplies and equipment. The Stowage, Configuration Analysis, and Operations Planning teams collaborate to perform the bulk of that planning. A Geometric Reasoning Engine is developed in a way that can be shared by the teams to optimize item placement in the context of crew planning.

The ISS crew spends (at the time of this writing) a third or more of their time moving supplies and equipment around. Better logistical support and optimized packing could make a significant impact on operational efficiency of the ISS. Currently, computational geometry and motion planning do not focus specifically on the optimized orientation and placement of 3D objects based on multiple distance and containment preferences and constraints.

The software performs reasoning about the manipulation of 3D solid models in order to maximize an objective function based on distance. It optimizes for 3D orientation and placement. Spatial placement optimization is a general problem and can be applied to object packing or asset relocation.

This work was done by Bradley J. Clement and Russell L. Knight of Caltech for NASA's Jet Propulsion Laboratory. Further information is contained in a TSP (see page 1).

This software is available for commercial licensing. Please contact Daniel Broderick of the California Institute of Technology at danielb@caltech.edu. Refer to NPO-47436.

⊚ Water Detection Based on Color Variation

This software has been designed to detect water bodies that are out in the open on cross-country terrain at close range (out to 30 meters), using imagery acquired from a stereo pair of color cameras mounted on a terrestrial, unmanned ground vehicle (UGV). This detector exploits the fact that the color variation across water bodies is generally larger and more uniform than that of other naturally occurring types of terrain, such as soil and vegetation. Non-traversable water bodies, such as large puddles, ponds, and lakes, are detected based on color variation, image intensity variance, image intensity gradient, size, and shape.

At ranges beyond 20 meters, water bodies out in the open can be indirectly detected by detecting reflections of the sky below the horizon in color imagery. But at closer range, the color coming out of a water body dominates sky reflections, and the water cue from sky reflections is of marginal use. Since there may be times during UGV autonomous navigation when a water body does not come into a perception system's field of view until it is at close range, the ability to detect water bodies at close range is critical. Factors that influence the perceived color of a water body at close range are the amount and type of sediment in the water, the water's depth, and the angle of incidence to the water body. Developing a single model of the mixture ratio of light reflected off the water surface (to the camera) to light coming out of the water body (to the camera) for all water bodies would be fairly difficult. Instead, this software detects close water bodies based on local terrain features and the natural, uniform change in color that occurs across the surface from the leading edge to the trailing edge.

From a water body's leading edge to the trailing edge, brightness and saturation levels tend to increase, with saturation content changing at a faster rate than the brightness content. For all the pixels on a water body, a plot of brightness/saturation vs. incidence angle is fairly linear with high slope. Fortuitously, this slope tends to be higher for water than other naturally occurring terrain. This phenomenology was exploited here to develop software that detects water bodies at close range. First, candidate water regions are identified in image space by locating regions having low texture. Next, the color changes are evaluated across each candidate water region to locate those consistent with water. Finally, an ellipse fit is performed on remaining candidate water regions and size and aspect ratio filtering is applied to prune regions that geometrically are not likely to be water.

This work was done by Arturo L. Rankin of Caltech for NASA's Jet Propulsion Laboratory. Further information is contained in a TSP (see page 1).

Single-Layer, All-Metal Patch Antenna Element With Wide Bandwidth

This design is suitable for military and commercial environments with high ESD susceptibility.

NASA's Jet Propulsion Laboratory, Pasadena, California

It is known that the impedance at the center of a patch antenna element is a short circuit, implying that a wire or post can be connected from the patch to the groundplane at this point without impacting radiation performance. In principle, this central post can be used to support the patch element, thus eliminating the need for dielectric. In spaceborne applications, this approach is problematic because a patch element supported by a single, thin post is highly susceptible to acoustic loads during launch.

The technology reported here uses a large-diameter center post as its supporting structure. The supporting structure allows for the fabrication of a sufficiently rigid antenna element that can survive launch loads. The post may be either hollow or solid, depending on fabrication approach and/or mass constraints. The patch antenna element and support post are envisioned as being fabricated (milled) from a single piece of aluminum or other metal. Alternately, the patch plate and support column can be fabricated separately and then joined using fasteners, adhesive, or welding. Casting and electroforming are also viable techniques for manufacturing the metal patch part(s). The patch structure is then either bonded or fastened to the

supporting groundplane. Arrays of patch elements can be fabricated by attaching several structures to a common groundplane/support structure.

Patch antennas can be fed in a number of different ways; the current design is envisioned as being fed from a coaxial probe, the connector of which is attached to the backside of a supporting groundplane. The probe can be either soldered to the patch or attached by means of a slip-fit connector assembly in the patch. The latter approach provides stress relief for the probe attachment during launch. The thickness of the patch material, interconnect technique, and attachment technique will depend on individual mass and launch load requirements. Alternatively, techniques such as aperture coupling or proximity coupling could be used to feed the patch.

The all-metal design eliminates the use of dielectric in patch substrate, making it suitable to environments with high electrostatic discharge (ESD) susceptibility. Elimination of dielectric also makes the tuning of the element largely independent of material properties (principally permittivity) and eliminates dielectric losses, which become appreciable at high frequencies. This simplifies the design and modeling of the antenna element. Concurrence between

measurements and modeling is thus driven by the fidelity of the modeling software and fabrication tolerances (as opposed to material properties). Additionally, the large central support column has been shown to increase the bandwidth of the element to 20% without significantly affecting the radiation pattern performance. Typically, a stacked patch design is used to obtain an impedance bandwidth of 20% or more. While the new technology was conceived for the purpose of eliminating dielectric from the patch-radiating element, a large-diameter ground post could be added to dielectric-based patch designs to increase bandwidth without having to add extra radiating layers. The new design has good cross-polarization suppression (better than 50 dB) because of the symmetry of the design.

This work was done by Neil F. Chamberlain, Richard E. Hodges, and Mark S. Zawadzki of Caltech for NASA's Jet Propulsion Laboratory. For more information, contact iaoffice@jpl.nasa.gov.

This invention is owned by NASA, and a patent application has been filed. Inquiries concerning nonexclusive or exclusive license for its commercial development should be addressed to the Patent Counsel, NASA Management Office–JPL. Refer to NPO-46843.

Scanning Laser Infrared Molecular Spectrometer (SLIMS)

This instrument can be used in any application requiring chemical sensing.

NASA's Jet Propulsion Laboratory, Pasadena, California

This prototype innovation is a novel design that achieves very long, effective laser path lengths that are able to yield ppb (parts per billion) and sub-ppb measurements of trace gases. SLIMS can also accommodate multiple laser channels covering a wide range of wavelengths, resulting in detection of more chemicals of interest. The me-

chanical design of the mirror cell allows for the large effective path length within a small footprint. The same design provides a robust structure that lends itself to being immune to some of the alignment challenges that similar cells face.

By taking a hollow cylinder and by cutting an elliptically or spherically curved

surface into its inner wall, the basic geometry of a reflecting ring is created. If the curved, inner surface is diamond-turned and highly polished, a surface that is very highly reflective can be formed. The surface finish can be further improved by adding a thin chrome or gold film over the surface. This creates a high-quality, curved, mirrored sur-

face. A laser beam, which can be injected from a small bore hole in the wall of the cylinder, will be able to make many low-loss bounces around the ring, creating a large optical path length.

The reflecting ring operates on the same principle as the Herriott cell. The difference exists in the mirror that doesn't have to be optically aligned, and which has a relatively large, internal surface area that lends itself to either open air or evacuated spectroscopic measurements. This solid, spherical ring mirror removes the possibility of mirror misalignment caused by thermal expansion or vibrations, because there is only a single, solid reflecting surface. Benefits of the reflecting ring come into play when size constraints reduce the size of the system, especially for space missions in which mass is at a premium.

This work was done by David C. Scott, Kelly Rickey, Alexander Ksendzov, Warren P. George, and Abdullah S. Aljabri of Caltech; and Joel M. Steinkraus of Cal Poly for NASA's Jet Propulsion Laboratory. Further information is contained in a TSP (see page 1).

➋ Next-Generation Microshutter Arrays for Large-Format Imaging and Spectroscopy

Goddard Space Flight Center, Greenbelt, Maryland

A next-generation microshutter array, LArge Microshutter Array (LAMA), was developed as a multi-object field selector. LAMA consists of small-scaled microshutter arrays that can be combined to form large-scale microshutter array mosaics. Microshutter actuation is accomplished via electrostatic attraction between the shutter and a counter electrode, and 2D addressing can be accomplished by applying an electrostatic potential between a row of shutters and a column, orthogonal to the row, of counter electrodes. Microelectromechanical system (MEMS) technology is used to fabricate the microshutter arrays.

The main feature of the microshutter device is to use a set of standard surface micromachining processes for device fabrication. Electrostatic actuation is used to eliminate the need for macro-mechanical magnet actuating components. A simplified electrostatic actuation with no macro components (e.g. moving magnets) required for actuation and latching of the shutters will make the microshutter arrays robust and less prone to mechanical failure. Smaller-size individual arrays will help to increase the yield and thus reduce the cost and improve robustness of the fabrication process. Reducing the size of the individual shutter array to about one square inch and building the large-scale mosaics by tiling these smaller-size arrays would further help to reduce the cost of the device due to the higher yield of smaller devices.

The LAMA development is based on prior experience acquired while developing microshutter arrays for the James Webb Space Telescope (JWST), but it will have different features. The LAMA modular design permits large-format mosaicking to cover a field of view at least 50 times larger than JWST MSA. The LAMA electrostatic, instead of magnetic, actuation enables operation cycles at least 100 times faster and a mass significantly smaller compared to JWST MSA. Also, standard surface micromachining technology will simplify the fabrication process, increasing yield and reducing cost.

This work was done by Samuel Moseley, Alexander Kutyrev, Ari Brown, and Mary Li of Goddard Space Flight Center. Further information is contained in a TSP (see page 1). GSC-16000-1

Materials & Coatings

Detection of Carbon Monoxide Using Polymer-Composite Films With a Porphyrin-Functionalized Polypyrrole

This technique can be used in home safety applications, first-responder safety, fire detection, and fire cleanup.

NASA's Jet Propulsion Laboratory, Pasadena, California

Post-fire air constituents that are of interest to NASA include CO and some acid gases (HCl and HCN). CO is an important analyte to be able to sense in human habitats since it is a marker for both pre-fire detection and post-fire cleanup.

The need exists for a sensor that can be incorporated into an existing sensing array architecture. The CO sensor needs to be a low-power chemiresistor that operates at room temperature; the sensor fabrication techniques must be compatible with ceramic substrates. Early work on the JPL ElectronicNose indicated that some of the existing polymer-carbon black sensors might be suitable. In addition, the CO sensor based on polypyrrole functionalized with iron porphyrin was demonstrated to be a promising sensor that could meet the requirements.

First, pyrrole was polymerized in a ferric chloride/iron porphyrin solution in methanol. The iron porphyrin is 5, 10, 15, 20-tetraphenyl-21H, 23H-porphine iron (III) chloride. This creates a polypyrrole that is functionalized with the porphyrin. After synthesis, the polymer is dried in an oven. Sensors were made from the functionalized polypyrrole by binding it with a small amount of polyethylene oxide (600 MW). This composite made films that were too resistive to be measured in the device.

Subsequently, carbon black was added to the composite to bring the sensing film resistivity within a measurable range. A suspension was created in methanol using the functionalized polypyrrole (90% by weight), polyethylene oxide (600,000 MW, 5% by weight), and carbon black (5% by weight). The sensing films were then deposited, like the polymer-carbon black sensors. After deposition, the substrates were dried in a vacuum oven for four hours at 60 °C. These sensors showed good response to CO at concentrations over 100 ppm.

While the sensor is based on a functionalized pyrrole, the actual composite is more robust and flexible. A polymer binder was added to help keep the sensor material from delaminating from the electrodes, and carbon was added to improve the conductivity of the material.

Enhanced-Adhesion Multiwalled Carbon Nanotubes on Titanium Substrates for Stray Light Control

Commercial applications include telescopes, binoculars, night vision goggles, and other optical devices that benefit from stray light suppression.

Goddard Space Flight Center, Greenbelt, Maryland

Carbon nanotubes previously grown on silicon have extremely low reflectance, making them a good candidate for stray light suppression. Silicon, however, is not a good structural material for stray light components such as tubes, stops, and baffles. Titanium is a good structural material and can tolerate the 700 °C nanotube growth process.

The ability to grow carbon nanotubes on a titanium substrate that are ten times blacker than the current NASA state-of-the-art paints in the visible to near infrared spectra has been achieved. This innovation will allow significant improvement of stray light performance in scientific instruments or any other optical system. This innovation is a refinement of the utilization of multiwalled carbon nanotubes for stray light suppression in spaceflight instruments. The innovation is a process to make the surface darker and improve the adhesion to the substrate, improving robustness for spaceflight use.

Bright objects such as clouds or ice scatter light off of instrument structures and components and make it difficult to see dim objects in Earth observations. A darker material to suppress this stray light has multiple benefits to these observations, including enabling scientific observations not currently possible, increasing observational efficiencies in high-contrast scenes, and simplifying instruments and lowering their cost by utilizing fewer stray light components and achieving equivalent performance.

The prior art was to use commercially available black paint, which resulted in approximately 4% of the light being reflected (hemispherical reflectance or total integrated scatter, or TIS). Use of multiwalled carbon nanotubes on titanium components such as baffles, entrance aperture, tubes, and stops, can decrease this scattered light by a factor of ten per bounce over the 200-nm to 2,500-nm wavelength range. This can improve system stray light performance by orders of magnitude.

The purpose of the innovation is to provide an enhanced stray light control capability by making a blacker surface treatment for typical stray light control components. Since baffles, stops, and tubes used in scientific observations often undergo loads such as vibration, it was critical to develop this surface treatment on structural materials. The innovation is to optimize the carbon nanotube growth for titanium, which is a strong, lightweight structural material suitable for spaceflight use.

The titanium substrate carbon nanotubes are more robust than those grown on silicon and allow for easier utilization. They are darker than current surface treatments over larger angles and larger wavelength range. The primary advantage of titanium substrate is that it is a good structural material, and not as brittle as silicon.

Three-Dimensional Porous Particles Composed of Curved, Two-Dimensional, Nano-Sized Layers for Li-Ion Batteries

A new method and materials were developed for preparing high-performance Si-based anodes for secondary Li-ion batteries.

John H. Glenn Research Center, Cleveland, Ohio

Building on previous knowledge acquired through research on thin-film batteries, three-dimensional (3D) porous macroscopic particles consisting of curved two-dimensional (2D) nanostructures of Si may bring unique advantages for Si anode technology. Prior work on thin Si films showed that during Li insertion, large-area Si films mostly accommodate the volume changes via variation in thickness. Therefore, the changes in the external surface area can fundamentally be minimized and thus, formation of a stable, solid electrolyte interphase (SEI) should be easier to achieve. In contrast, Si nanoparticles expand uniformly in all dimensions and thus, their outer surface area (where SEI forms) changes dramatically during insertion/extraction of Si. The low elasticity of the SEI makes it difficult to achieve the long-term stability under cycling load. Further, thin Si films have lower surface area (for the same mass), in comparison to Si nanoparticles, and better potential for achieving low irreversible capacity losses on the first and subsequent cycles.

Thin Si films coated on porous 3D particles composed of curved 2D graphene sheets have been synthesized utilizing techniques that allow for tunable properties. Since graphene exhibits specific surface area up to 100 times higher than carbon black or graphite, the deposition of the same mass of Si on graphene is much faster in comparison — a factor which is important for practical applications. In addition, the distance between graphene layers is tunable and variation in the thickness of the deposited Si film is feasible. Both of these characteristics allow for optimization of the energy and power characteristics. Thicker films will allow higher capacity, but slower rate capabilities. Thinner films will allow more rapid charging, or higher power performance.

In this innovation, uniform deposition of Si and C layers on high-surface-area graphene produced granules with specific surface area (SSA) of ≈ 5 m^{2}g^{-1}. The over 100 times reduction in SSA of the initial graphene material is important for high Coulombic efficiencies on the first and subsequent cycles. Here, the low surface area of the composite resulted in an average Coulombic effi-
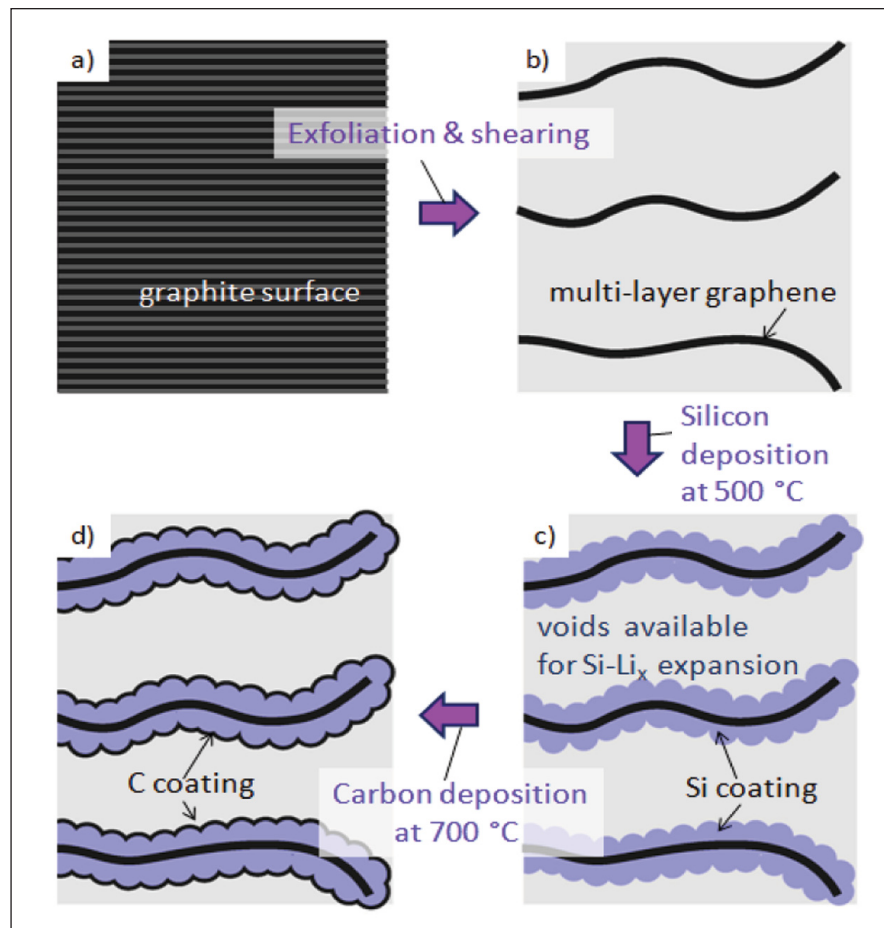
A schematic of **C-Si-Graphene Composite Formation**: (a) natural graphite is transformed to (b) graphene, and then (c) coated by Si nanoparticles and (d) a thin C layer.

ciency in excess of 99%. The anode composed of the nanocomposite particles exhibited specific capacity in excess of 2,000 mAhg^{-1} at the current density of 140 mAg^{-1} and excellent stability for 150 cycles, significantly exceeding the theoretical capacity of graphite and graphene. While only a Si-containing composite was demonstrated, the synthesis techniques utilized are applicable for other high-capacity materials that can be conformally coated on graphene. Similarly, while only curved graphene was used as a substrate for Si deposition, other curved, thin, 2D substrates (which do not react with Si precursors) may be used for conformal coating by Si or other high-capacity materials.

This work was performed by Gleb Yushin, Kara Evanoff, and Alexander Magasinski of

Ultra-Lightweight Nanocomposite Foams and Sandwich Structures for Space Structure Applications

Marshall Space Flight Center, Alabama

Microcellular nanocomposite foams and sandwich structures have been created to have excellent electrical conductivity and radiation-resistant properties using a new method that does not involve or release any toxicity. The nanocomposite structures have been scaled up in size to 12×12 in. (30×30 cm) for components fabrication. These sandwich materials were fabricated mainly from PE, CNF, and carbon fibers. Test results indicate that they have very good compression and compression-after-impact properties, excellent electrical conductivity, and superior space environment durability.

Compression tests show that 1000 ESH (equivalent Sun hours) of UV exposure has no effect on the structural properties of the sandwich structures. The structures are considerably lighter than aluminum alloy (≈36 percent lighter), which translates to 36 percent weight savings of the electronic enclosure and its housing. The good mechanical properties of the materials may enable the electronic housing to be fabricated with a thinner structure that further reduces the weight. There was no difficulty in machining the sandwich specimens into electronic enclosure housing.

Thermally Resilient, Broadband Optical Absorber From UV to IR Derived From Carbon Nanostructures

This technology can be used in aerospace, semiconductors, antireflection coatings, optoelectronics, and communications.

NASA's Jet Propulsion Laboratory, Pasadena, California

Optical absorber coatings have been developed from carbon-based paints, metal blacks, or glassy carbon. However, such materials are not truly black and have poor absorption characteristics at longer wavelengths. The blackness of such coatings is important to increase the accuracy of calibration targets used in radiometric imaging spectrometers since blackbody cavities are prohibitively large in size. Such coatings are also useful potentially for thermal detectors, where a broadband absorber is desired. Au-black has been a commonly used broadband optical absorber, but it is very fragile and can easily be damaged by heat and mechanical vibration. An optically efficient, thermally rugged absorber could also be beneficial for thermal solar cell applications for energy harnessing, particularly in the 350–2,500 nm spectral window.

It has been demonstrated that arrays of vertically oriented carbon nanotubes (CNTs), specifically multi-walled-carbon-nanotubes (MWCNTs), are an exceptional optical absorber over a broad range of wavelengths well into the infrared (IR). The reflectance of such arrays is 100× lower compared to conventional black materials, such as Au black in the spectral window of 350–2,500 nm. Total hemispherical measurements revealed a reflectance of ≈1.7 % at λ ≈1 μm, and at longer wavelengths into the infrared (IR), the specular reflectance was ≈2.4 % at λ ≈7 μm.

The previously synthesized CNTs for optical absorber applications were formed using water-assisted thermal chemical vapor deposition (CVD), which yields CNT lengths in excess of 100's of microns. Vertical alignment, deemed to be a critical feature in enabling the high optical absorption from CNT arrays, occurs primarily via the crowding effect with thermal CVD synthesized CNTs, which is generally not effective in aligning CNTs with lengths < 10 μm. Here it has been shown that the electric field inherent in a plasma yields vertically aligned CNTs at small length scales (<10 μm), which still exhibit broadband, and high-efficiency optical absorption characteristics from the ultraviolet (UV) to IR. A thin and yet highly absorbing coating is extremely valuable for detector applications for radiometry in order to enhance sensitivity. A plasma-based process also increases

the potential of forming the optical absorbers at lower synthesis temperatures in the future, increasing the prospects of integrating the absorbers with flexible substrates for low-cost solar cell applications, for example.

Loading, Release, Biodegradation, and Biocompatibility of a Nanovector Delivery System

This method enables targeted delivery of therapeutic or imaging agents within a patient by means of nested nanoparticles.

Lyndon B. Johnson Space Center, Houston, Texas

A nanovector multistage system has been created to overcome or bypass sequential barriers within the human body, in order to deliver a therapeutic or imaging agent to a specific location. This innovation consists of a composition that includes two or more stages of particles, such that smaller, later-stage particles are contained in the larger, early-stage particles (see figure).

Such multistage compositions provide several advantages. An active agent, such as a therapeutic agent or imaging agent, is preferentially delivered and/or localized to a particular target site in the body of a subject. The multistage composition overcomes multiple biological barriers in the body. The multistage composition also allows for simultaneous delivery and localization at the same or different target sites of multiple active agents.

Following administration, an active agent formulated conventionally, or in a nanovector, encounters a number of biological barriers that adversely impact the agent's ability to reach an intended target at a desired location. Because these barriers are sequential, the method for overcoming or bypassing them has to be sequential as well. In this innovation, each stage of the vehicle is defined by a particle having a separate intended function, which may be different from an intended function of a particle of another stage. For example, a particle of one stage is designed to target a specific body site, which may be different from a site targeted by a particle of another stage.

A particle of each subsequent stage is contained inside a particle of an immediately preceding stage. A particle of any particular stage may contain an active agent, such as the therapeutic agent or an imaging agent, intended for use at this particular stage. The number and type of stages in the multistage delivery vehicle depends on several parameters, including administra-
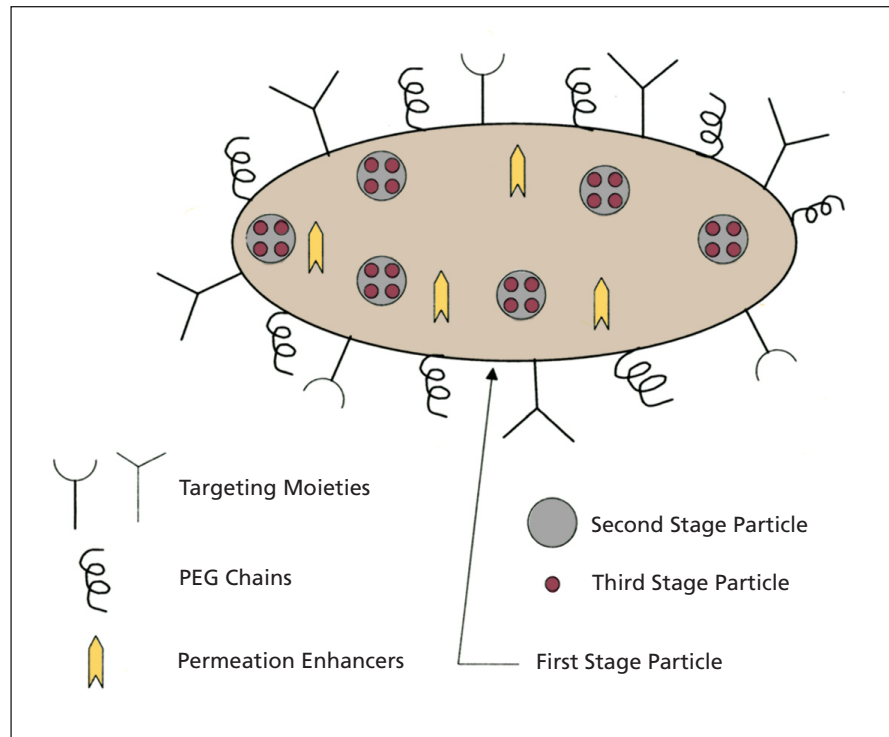
In the **Multistage Delivery Vehicle**, the first-stage particle contains second-stage particles and an additional agent such as an imaging or therapeutic agent. The second-stage particles may contain third-stage particles. Targeting moieties such as antibodies attached to the first-stage particle facilitate localization at the selected body site.

tion route and an intended final target for the active agent.

Sometimes, the particle of the first stage is a micro or nano particle. Other times, the first-stage particle has a characteristic size of at least 500 µm, or at least 1 mm. Such a particle may be configured to contain inside at least one micro or nano particle, which, in turn, may contain inside at least one particle of a smaller size. The first stage particle is a top-down fabricated particle, i.e., a particle prepared by top-down microfabrication or nanofabrication methods, such as photolithography, electron beam lithography, X-ray lithography, deep UV lithography, or nanoprint lithography. A potential advantage of using the top-down fabrication methods is that such methods

provide for a scaled-up production of particles that are uniform in dimensions.

This work was done by Mauro Ferrari and Ennio Tasciotti of the University of Texas Health Science Center at Houston for Johnson Space Center. For further information, contact the JSC Innovation Partnership Office at (281) 483-3809.

In accordance with Public Law 96-517, the contractor has elected to retain title to this invention. Inquiries concerning rights for its commercial use should be addressed to:

The University of Texas
Health Science Center at Houston
1825 Pressler, Suite 537D
Houston. TX 77030
Refer to MSC-24478-1, volume and number of this NASA Tech Briefs *issue, and the page number.*

Hardy Bacterium Isolated From Two Geographically Distinct Spacecraft Assembly Cleanroom Facilities

A new species merits further study.

NASA's Jet Propulsion Laboratory, Pasadena, California

Earlier studies have confirmed that a tenacious hardy bacterial population manages to persist and survive throughout a spacecraft assembly process. The widespread detection of these organisms underscores the challenges in eliminating them completely. Only comprehensive and repetitive microbial diversity studies of geographically distinct cleanroom facilities will bolster the understanding of planetary protection relevant microbes. Extensive characterizations of the physiological traits demonstrated by cleanroom microbes will aid NASA in gauging the forward contamination risk that hardy bacteria (such as *Tersicoccus phoenicis*) pose to spacecraft.

Rigorous standards are in place for the cleaning and monitoring of spacecraft assembly environments to help minimize the inadvertent forward contamination by microorganisms during space missions. Cleanroom environments are oligotrophic (low-nutrient level), desiccated (humidity controlled), certified to a defined low particle concentration, and maintained at constant temperature. Yet despite these unfavorable conditions, a subset of tenacious microbes is known to exist in these assembly facilities.

This study reports on the isolation and identification of two gram-positive, non-motile, non-spore-forming bacterial strains from the spacecraft assembly facilities at Kennedy Space Center, Florida, USA and Centre Spatial Guyanais, Kourou, French Guiana. DNA-DNA relatedness values between the novel strains indicates that these novel strains were indeed members of a same species. Phylogenetic evidence derived from a 16S ribosomal DNA analysis indicated that both the novel strains are less closely related to all other *Arthrobacter* species. Based on phylogenetic and phenotypic results, it is concluded that these strains represent a new species of the novel genus *Tersicoccus*, for which the name *Tersicoccus phoenicis* sp. nov. is proposed. The presence of *Tersicoccus phoenicis* exclusively in the cleanroom environments from two distinct geographical locations suggests selective adaptation and a significant role for these microorganisms in these environments.

Microbes residing in the cleanrooms during the spacecraft assembly process could gain access to a spacecraft, and possibly survive en route to extraterrestrial systems. *Tersicoccus* and members of the *Arthrobacter* genus are metabolically versatile, producing many different enzymes allowing them to grow on a wide range of substrates, including agricultural pesticides, radioactive waste, and high concentration of toxic pollutant. Previously undescribed *Tersicoccus phoenicis*, isolated from two distinct cleanroom facilities, may exhibit even greater resilience than other microbial strains due to their selective adaptation to cleanroom environments. Thus, it is in the best interest of NASA to characterize this organism thoroughly, which will further assess in determining the potential for forward contamination and development of more effective bioburden reduction, cleaning, and sterilization technologies.

◎ Dual Double-Wedge Pseudo-Depolarizer With Anamorphic PSF

Potential commercial applications include imaging spectrometers, radiometers, and polarimeters.

Goddard Space Flight Center, Greenbelt, Maryland

A polarized scene, which may occur at oblique illumination angles, creates a radiometric signal that varies as a function of viewing angle. One common optical component that is used to minimize such an effect is a polarization scrambler or depolarizer. As part of the CLARREO mission, the SOLARIS instrument project at Goddard Space Flight Center has developed a new class of polarization scramblers using a dual double-wedge pseudo-depolarizer that produces an anamorphic point spread function (PSF).

The SOLARIS instrument uses two Wollaston type scramblers in series, each with a distinct wedge angle, to image a pseudo-depolarized scene that is free of eigenstates. Since each wedge is distinct, the scrambler is able to produce an anamorphic PSF that maintains high spatial resolution in one dimension by sacrificing the spatial resolution in the other dimension. This scrambler geometry is ideal for 1-D imagers, such as pushbroom slit spectrometers, which require high spectral resolution, high spatial resolution, and low sensitivity to polarized light. Moreover, the geometry is applicable to a wide range of scientific instruments that require both high SNR (signal-to-noise ratio) and low sensitivity to polarized scenes.

Classic polarization scramblers are built using birefringent glass that may be either air-spaced or optically contacted together. Examples of birefringent materials include quartz, magnesium fluoride, and calcite. Two popular design forms of polarization scramblers are the Lyot and Wollaston types. The Lyot type uses two plan parallel birefringent plates of different thicknesses to vary the polarization state as a function of wavelength. Integrating the scene across a broad spectrum scrambles the polarized scene. This type reduces the spectral resolution of the scene. The Wollaston type uses two wedged birefringent plates to scramble the polarization state spatially. This type reduces the image quality of the scene. In addition to reducing the image quality of the scene, a single Wollaston scrambler is known to have polarized eigenstates and is ineffective at scrambling certain polarized scenes.

The SOLARIS instrument is designed to measure the solar radiation reflected from the Earth. The design furthers the state of the art in UV to near IR imaging spectroscopy.

This work was done by Peter Hill and Patrick Thompson of Goddard Space Flight Center. Further information is contained in a TSP (see page 1). GSC-16277-1

◎ Cavitating Jet Method and System for Oxygenation of Liquids

Cavitation is considered to be more efficient in reclamation and re-use of water for space-based life support systems than sonochemistry.

Lyndon B. Johnson Space Center, Houston, Texas

Reclamation and re-use of water is critical for space-based life support systems. A number of functions must be performed by any such system including removal of various contaminants and oxygenation. For long-duration space missions, this must be done with a compact, reliable system that requires little or no use of expendables and minimal power. DynaJets cavitating jets can oxidize selected organic compounds with much greater energy efficiency than ultrasonic devices typically used in sonochemistry. The focus of this work was to develop cavitating jets to simultaneously accomplish the functions of oxygenation and removal of contaminants of importance to space-structured water reclamation systems.

The innovation is a method to increase the concentration of dissolved oxygen or other gasses in a liquid. It utilizes a particular form of novel cavitating jet operating at low to moderate pressures to achieve a high-efficiency means of transporting and mixing the gas into the liquid. When such a jet is utilized to simultaneously oxygenate the liquid and to oxidize organic compounds within the liquid, such as those in waste water, the rates of contaminant removal are increased.

The invention is directed toward an increase in the dissolved gas content of a liquid, in general, and the dissolved oxygen content of a liquid in particular. Liquid at moderate pressure is forced into a DynaSwirl swirl chamber in which a central vortex is formed that has a core pressure lower than the vapor pressure of the liquid, thus inducing cavitation in the vortex into which the desired gas(es) are drawn or injected. The cavitation is then ejected from the nozzle through the exit orifice into a volume of liquid where the cavities break up and collapse. The large cavity surface area and violent mixing due to cavity collapse are believed to facilitate gas transport and dissolution into the liquid. These cavitation events have also been found to drive chemical reactions in a manner similar to that of ultrasonic sonochemistry, efficiently decomposing and destroying contaminating organic compounds. The reactions have been found to proceed more rapidly in the presence of air injection or oxygenation by this means.

This work was done by Georges L. Chahine of Dynaflow, Inc. for Johnson Space Center. Further information is contained in a TSP (see page 1). MSC-24019-1

A Compact, High-Flux Cold Atom Beam Source

High atom loading efficiency is important for compact and mobile devices where laser power and space are limited.

NASA's Jet Propulsion Laboratory, Pasadena, California

The performance of cold atom experiments relying on three-dimensional magneto-optical trap techniques can be greatly enhanced by employing a high-flux cold atom beam to obtain high atom loading rates while maintaining low background pressures in the UHV MOT (ultra-high vacuum magneto-optical trap) regions. Several techniques exist for generating slow beams of cold atoms. However, one of the technically simplest approaches is a two-dimensional (2D) MOT. Such an atom source typically employs at least two orthogonal trapping beams, plus an additional longitudinal "push" beam to yield maximum atomic flux.

A 2D atom source was created with angled trapping collimators that not only traps atoms in two orthogonal directions, but also provides a longitudinal pushing component that eliminates the need for an additional push beam. This development reduces the overall package size, which in turn, makes the 2D trap simpler, and requires less total optical power. The atom source is more compact than a previously published effort, and has greater than an order of magnitude improved loading performance.

An effective pushing field component was realized by tilting the 2D MOT collimators towards a separate three-dimensional (3D) MOT in ultra-high vacuum. This technique significantly improved 3D MOT loading rates to greater than 8×10^9 atoms/s using only 20 mW of total laser power for the source. When operating below saturation, a maximum efficiency of 6.2×10^{11} atoms/s/W was achieved.

One of the most significant improvements of the present 2D MOT over conventional elliptical-beam 2D MOT designs is the angle of the collimators with respect to the axis of the 2D MOT. Both the horizontal and vertical collimators have been optimized to include forward tilt. Associated retro-mirrors are mounted parallel to the axis of the 2D MOT, thus insuring that the reflected beams are also projected forward at the same angle as the incident beams, effectively resulting in a pushing component with a fraction of the overall laser field in each orthogonal direction. The increased push factor at larger collimator angles is offset by reduced lateral trapping efficiency. It is worth noting that the intrinsic symmetry of a retro-reflected beam setup is very robust and simple to use.

The forward-angled collimator method allows for high 2D atomic flux without the need for an additional push laser and associated optical and electronic hardware. This cold atom source maintains very high efficiencies while utilizing a simpler, more compact, and more robust package than previous atom sources. The compact design and efficiency of the current apparatus is suitable for cold atom applications in the laboratory, and especially in mobile devices, including cold atom instruments in space.

This work was done by James R. Kellogg, James M. Kohel, Robert J. Thompson, David C. Aveline, and Nan Yu of Caltech; and Dennis Schlippert of the Institut für Quantenoptik, Hannover, Germany for NASA's Jet Propulsion Laboratory. For more information, contact iaoffice@jpl.nasa.gov. NPO-48322

Sample-Clock Phase-Control Feedback

The throughput of a pulse-position modulation with 16 slots can increase from 188 Mb/s to 1.5 Gb/s.

NASA's Jet Propulsion Laboratory, Pasadena, California

To demodulate a communication signal, a receiver must recover and synchronize to the symbol timing of a received waveform. In a system that utilizes digital sampling, the fidelity of synchronization is limited by the time between the symbol boundary and closest sample time location. To reduce this error, one typically uses a sample clock in excess of the symbol rate in order to provide multiple samples per symbol, thereby lowering the error limit to a fraction of a symbol time. For systems with a large modulation bandwidth, the required sample clock rate is prohibitive due to current technological barriers and processing complexity. With precise control of the phase of the sample clock, one can sample the received signal at times arbitrarily close to the symbol boundary, thus obviating the need, from a synchronization perspective, for multiple samples per symbol.

Sample-clock phase-control feedback was developed for use in the demodulation of an optical communication signal, where multi-GHz modulation bandwidths would require prohibitively large sample clock frequencies for rates in excess of the symbol rate. A custom mixed-signal (RF/digital) offset phase-locked loop circuit was developed to control the phase of the 6.4-GHz clock that samples the photon-counting detector output. The offset phase-locked loop is driven by a feedback mechanism that continuously corrects for variation in the symbol time due to motion between the transmitter and receiver as well as oscillator instability. This innovation will allow significant improvements in receiver throughput; for example, the throughput of a pulse-position modulation (PPM) with 16 slots can increase from 188 Mb/s to 1.5 Gb/s.

The novelty of this innovation is precise control of the sample-clock phase supports synchronization to the symbol timing of the received waveform without the use of a sample clock in excess of the symbol rate. This can reduce the required sample clock frequency for demodulation of a communication signal, and thereby reduce the processing complexity as well as permit demodulation of large bandwidth signals for which there was a technological barrier to a

sample frequency in excess of the symbol rate.

Sample-clock phase-control feedback has direct applications in optical and radio frequency communication systems for satellite and deep space applications, as well as other applications in high-precision timing.

This work was done by Kevin J. Quirk, Jonathan W. Gin, Danh H. Nguyen, and Huy Nguyen of Caltech for NASA's Jet Propulsion Laboratory. Further information is contained in a TSP (see page 1). NPO-47663

360° Camera Head for Unmanned Sea Surface Vehicles

NASA's Jet Propulsion Laboratory, Pasadena, California

Autonomous navigation and control for unmanned sea surface vehicles requires a visual sensing system to provide a 360° view from the vehicle deck for situational awareness. Successful operation required a sensing system mechanically packaged to withstand weather, sea spray, and an environment of continual motion and mechanical shock. A low-cost, easily manufacturable, watertight, and mechanically robust sensing system was developed for autonomous navigation and intelligent control.

The 360° camera head consists of a set of six color cameras arranged in a circular pattern such that their overlapping fields of view give a full 360° view of the immediate surroundings. The cameras are enclosed in a watertight container along with support electronics and a power distribution system. Each camera views the world through a watertight porthole. To prevent overheating or condensation in extreme weather conditions, the watertight container is also equipped with an electrical cooling unit and a pair of internal fans for circulation.

Most JPL systems use cameras that are pointed at targets either through actuation or motion of the host vehicle. The 360° six-camera layout allows full situational awareness in all directions with no actuation required. Also novel is the watertight design, which encases all six cameras in a cylinder with six symmetrically placed windows. Each window employs a porthole-style design, in which the circular glass pane is sealed against an O-ring to prevent leaking. All cylinder access panels are similarly sealed with O-rings, and the electrical cooling unit, which sits half inside and half outside the camera head, is sealed with closed cell silicone foam.

This design proves the utility of 360° visual sensing to enhance situational awareness for Naval Unmanned Sea Surface Forces. The concept could be applied to future space missions to increase visual situational awareness without increasing actuation requirements.

This work was done by Julie A. Townsend, Eric A. Kulczycki, Reginald G. Willson, Terrance L. Huntsberger, Michael S. Garrett, Ashitey Trebi-Ollennu, and Charles F. Bergh of Caltech for NASA's Jet Propulsion Laboratory. For more information, contact iaoffice@jpl.nasa.gov.

This invention is owned by NASA, and a patent application has been filed. Inquiries concerning nonexclusive or exclusive license for its commercial development should be addressed to the Patent Counsel, NASA Management Office–JPL. Refer to NPO-47717.

Microgravity Passive Phase Separator

There are no moving parts and there are no failure modes that involve fluid loss.

Lyndon B. Johnson Space Center, Houston, Texas

A new invention disclosure discusses a structure and process for separating gas from liquids in microgravity. The Microgravity Passive Phase Separator consists of two concentric, pleated, woven stainless-steel screens (25-μm nominal pore) with an axial inlet, and an annular outlet between both screens (see figure). Water enters at one end of the center screen at high velocity, eventually passing through the inner screen and out through the annular exit. As gas is introduced into the flow stream, the drag force exerted on the bubble pushes it downstream until flow stagnation or until it reaches an equilibrium point between the surface tension holding bubble to the screen and the drag force.

Gas bubbles of a given size will form a "front" that is moved further down the
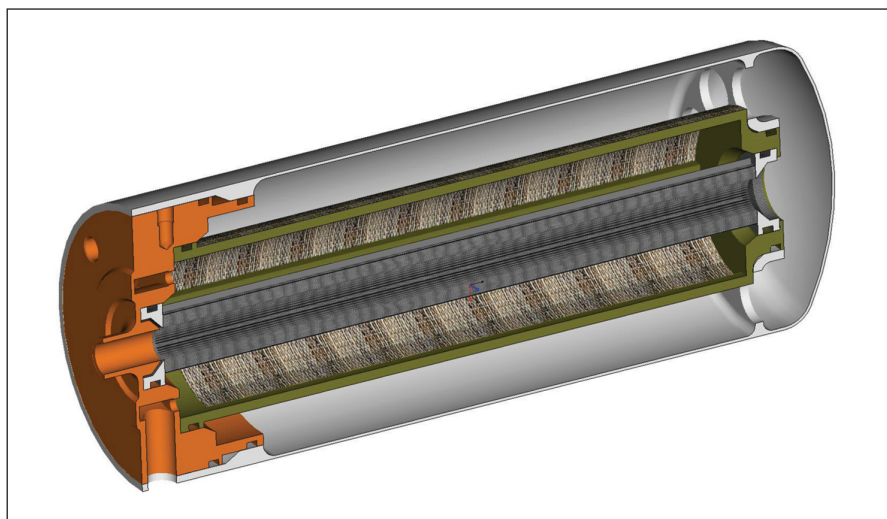
Microgravity Passive Phase Separator

length of the inner screen with increasing velocity. As more bubbles are added, the front location will remain fixed, but additional bubbles will move to the end of the unit, eventually coming to rest in the large cavity between the unit housing and the outer screen (storage area). Owing to the small size of the pores and the hydrophilic nature of the screen material, gas does not pass through the screen and is retained within the unit for emptying during ground processing. If debris is picked up on the screen, the area closest to the inlet will become clogged, so high-velocity flow will persist farther down the length of the center screen, pushing the bubble front further from the inlet of the inner screen. It is desired to keep the velocity high enough so that, for any bubble size, an area of clean screen exists between the bubbles and the debris.

The primary benefits of this innovation are the lack of any need for additional power, strip gas, or location for venting the separated gas. As the unit contains no membrane, the transport fluid will not be lost due to evaporation in the process of gas separation. Separation is performed with relatively low pressure drop based on the large surface area of the separating screen. Additionally, there are no moving parts, and there are no failure modes that involve fluid loss. A patent application has been filed.

This work was done by Matthew Paragano, William Indoe, and Jeffrey Darmetko of

⊃ Verilog-A Device Models for Cryogenic Temperature Operation of Bulk Silicon CMOS Devices

These models can be used in cryogenic electronics applications such as cooled imagers and sensors, medical electronics, and remote sensing satellites.

Goddard Space Flight Center, Greenbelt, Maryland

Verilog-A based cryogenic bulk CMOS (complementary metal oxide semiconductor) compact models are built for state-of-the-art silicon CMOS processes. These models accurately predict device operation at cryogenic temperatures down to 4 K. The models are compatible with commercial circuit simulators. The models extend the standard BSIM4 [Berkeley Short-channel IGFET (insulated-gate field-effect transistor) Model] type compact models by re-parameterizing existing equations, as well as adding new equations that capture the physics of device operation at cryogenic temperatures. These models will allow circuit designers to create optimized, reliable, and robust circuits operating at cryogenic temperatures.

Circuits that operate reliably at cryogenic temperatures are very difficult to design, because reliable semiconductor device and circuit models are not available for these temperatures. The unique aspect of this problem is the unknown physical characteristics of devices operating at cryogenic temperatures. Standard circuit models such as BSIM4 contain equations that can only predict device op-

eration near room temperature. Therefore, new equations and re-parameterization of existing equations need to be done in order to functionalize the operation of state-of-the-art silicon CMOS devices at cryogenic temperatures.

These models will extend the room-temperature BSIM4 type compact models to temperatures as low as 4 K. The models are developed using the behavioral description language Verilog-A. Verilog-A allows for change in standard BSIM equations, re-parameterization of existing equations, and addition of new equations that capture the physics of semiconductor device operation at cryogenic temperatures.

Creation of these Verilog-A based cryogenic models requires the following:
a. Test chip with an array of devices fabricated in the process of interest or test data for the process;
b. Room and cryogenic temperature measurement of test chip;
c. First parameterization of BSIM4 model using room temperature data;
d. Verilog-A model parameterization using the developed equations and using the cryogenic temperature data;

e. Optimization of new model; and
f. Testing the new model by simulating test circuits and comparing them with measurements of circuits on the test chip.

Next, Verilog-A cryogenic CMOS device models are inserted into a simulator. Circuit simulations are run using the new models at temperatures as low as 4 K. These models work in conjunction with other standard compact models without causing any convergence or other errors in the circuit simulator.

The models can be further modified to include effects of radiation such as total ionizing dose at cold temperatures. These models will be able to predict long-term reliability of CMOS-based electronics operating under cryogenic temperatures in radiation-rich environments. The new models include the effect of threshold voltage variation at extreme cold temperatures and variation in mobility at cryogenic temperatures.

This work was done by Akin Akturk, Siddharth Potbhare, Neil Goldsman, and Michael Holloway of CoolCAD Electronics for Goddard Space Flight Center. Further information is contained in a TSP (see page 1). GSC-16112-1

⊃ Rapid Process to Generate Beam Envelopes for Optical System Analysis

Two models take less time to complete beam envelope analysis.

Goddard Space Flight Center, Greenbelt, Maryland

The task of evaluating obstructions in the optical throughput of an optical system requires the use of two disciplines, and hence, two models: optical models for the details of optical propagation, and mechanical models for determining the actual structure that exists in the optical system. Previous analysis methods for creating beam envelopes (or cones of light) for use in this obstruction analy-

sis were found to be cumbersome to calculate and take significant time and resources to complete. A new process was developed that takes less time to complete beam envelope analysis, is more accurate and less dependent upon manual node tracking to create the beam envelopes, and eases the burden on the mechanical CAD (computer-aided design) designers to form the beam solids.

This algorithm allows rapid generation of beam envelopes for optical system obstruction analysis. Ray trace information is taken from optical design software and used to generate CAD objects that represent the boundary of the beam envelopes for detailed analysis in mechanical CAD software.

Matlab is used to call ray trace data from the optical model for all fields and

entrance pupil points of interest. These are chosen to be the edge of each space, so that these rays produce the bounding volume for the beam. The x and y global coordinate data is collected on the surface planes of interest, typically an image of the field and entrance pupil internal of the optical system. This x and y coordinate data is then evaluated using a convex hull algorithm, which removes any internal points, which are unnecessary to produce the bounding volume of interest. At this point, tolerances can be applied to expand the size of either the field or aperture, depending on the allocations. Once this minimum set of coordinates on the pupil and field is obtained, a new set of rays is generated between the field plane and aperture plane (or vice-versa).

These rays are then evaluated at planes between the aperture and field, at a desired number of steps perceived necessary to build up the bounding volume or cone shape. At each plane, the ray coordinates are again evaluated using the convex hull algorithm to reduce the data to a minimal set. When all of the coordinates of interest are obtained for every plane of the propagation, the data is formatted into an *xyz* file suitable for FRED optical analysis software to import and create a STEP file of the data. This results in a spiral-like structure that is easily imported by mechanical CAD users who can then use an automated algorithm to wrap a skin around it and create a solid that represents the beam.

This work was done by Joseph Howard and Lenward Seals of Goddard Space Flight Center. Further information is contained in a TSP (see page 1). GSC-16176-1

High-Performance, Multi-Node File Copies and Checksums for Clustered File Systems

Ames Research Center, Moffett Field, California

Modern parallel file systems achieve high performance using a variety of techniques, such as striping files across multiple disks to increase aggregate I/O bandwidth and spreading disks across multiple servers to increase aggregate interconnect bandwidth. To achieve peak performance from such systems, it is typically necessary to utilize multiple concurrent readers/writers from multiple systems to overcome various single-system limitations, such as number of processors and network bandwidth. The standard cp and md5sum tools of GNU coreutils found on every modern Unix/Linux system, however, utilize a single execution thread on a single CPU core of a single system, and hence cannot take full advantage of the increased performance of clustered file systems.

Mcp and msum are drop-in replacements for the standard cp and md5sum programs that utilize multiple types of parallelism and other optimizations to achieve maximum copy and checksum performance on clustered file systems. Multi-threading is used to ensure that nodes are kept as busy as possible. Read/write parallelism allows individual operations of a single copy to be overlapped using asynchronous I/O. Multi-node cooperation allows different nodes to take part in the same copy/checksum. Split-file processing allows multiple threads to operate concurrently on the same file. Finally, hash trees allow inherently serial checksums to be performed in parallel.

Mcp and msum provide significant performance improvements over standard cp and md5sum using multiple types of parallelism and other optimizations. The total speed-ups from all improvements are significant. Mcp improves cp performance over 27×, msum improves md5sum performance almost 19×, and the combination of mcp and msum improves verified copies via cp and md5sum by almost 22×. These improvements come in the form of drop-in replacements for cp and md5sum, so are easily used and are available for download as open source software at http://mutil.sourceforge.net.

This work was done by Paul Z. Kolano and Robert B. Ciotti of Ames Research Center. Further information is contained in a TSP (see page 1). ARC-16494-1

Stiffness and Damping Coefficient Estimation of Compliant Surface Gas Bearings for Oil-Free Turbomachinery
Initial applications include design of turbochargers, blowers, compressors, pumps, and turbine engines.

John H. Glenn Research Center, Cleveland, Ohio

Foil gas bearings are a key technology in many commercial and emerging oil-free turbomachinery systems. These bearings are nonlinear and have been difficult to analytically model in terms of performance characteristics such as load capacity, power loss, stiffness, and damping. Previous investigations led to an empirically derived method to estimate load capacity. This method has been a valuable tool in system development. The current work extends this tool concept to include rules for stiffness and damping coefficient estimation. It is expected that these rules will further accelerate the development and deployment of advanced oil-free machines operating on foil gas bearings.

Foil gas bearings are self-acting hydrodynamic bearings comprised of a series of sheet-metal foil layers from which they derive their name. They are compliant bearings that offer high-speed rotor support while accommodating shaft misalignment and distortion often encountered in turbomachinery. Lightly loaded, low-temperature foil gas bearings are commodities that predominate in the rotor support for aircraft air cycle machines (ACMs). More highly loaded foil

bearings operating at high temperatures are an emerging technology making commercial inroads into several markets including aircraft auxiliary power units (APUs), microturbines, gas compressors and blowers, and turbochargers.

The general trend for foil bearings since their initial development over five decades ago is application to larger and more complex rotor systems. As this proliferation occurs, more practitioners will become actively involved with new machine development using foil bearings. Thus, there is a great need for application guidelines to establish the feasibility of proposed rotor systems and to identify existing machines that are good candidates for foil bearing use. Specifically, a method is needed to estimate foil bearing stiffness and damping behavior in order to foster advanced oil-free rotating machine development.

Methods to estimate critical stiffness and damping parameters, however, do not currently exist. The purpose of the methods put forth in this work is to establish simple tools capable of estimating foil bearing stiffness and damping coefficients suitable for oil-free rotor support design work. This has been accomplished by first coalescing all available empirical data on foil bearing performance that has been generated in the author's own laboratories, and by researchers working in university, government, and industrial laboratories. This information is examined and combined, then used to develop ROT for foil bearing stiffness and damping. These ROTs can then be combined with existing rules for load capacity to obtain credible feasibility assessments for proposed oil-free rotor systems.

The effort described has resulted in algebraic models for foil gas bearings that yield stiffness, damping, and load capacity values as a function of bearing size, design, and operating speed. With these models, one can easily determine the feasibility of building a foil bearing supported machine without incurring the expense of early experimental work. The models presented represent the only known and verified methods to predict conveniently foil bearing performance properties.

This work was done by Christopher Della-Corte of Glenn Research Center. Further information is contained in a TSP (see page 1).

Inquiries concerning rights for the commercial use of this invention should be addressed to NASA Glenn Research Center, Innovative Partnerships Office, Attn: Steven Fedor, Mail Stop 4–8, 21000 Brookpark Road, Cleveland, Ohio 44135. Refer to LEW-18755-1.

Sampling and Reconstruction of the Pupil and Electric Field for Phase Retrieval

Goddard Space Flight Center, Greenbelt, Maryland

This technology is based on sampling considerations for a band-limited function, which has application to optical estimation generally, and to phase retrieval specifically. The analysis begins with the observation that the Fourier transform of an optical aperture function (pupil) can be implemented with minimal aliasing for Q values down to $Q = 1$. The sampling ratio, Q, is defined as the ratio of the sampling frequency to the band-limited cut-off frequency. The analytical results are given using a 1-d aperture function, and with the electric field defined by the band-limited $\text{sinc}(x)$ function. Perfect reconstruction of the Fourier transform (electric field) is derived using the Whittaker-Shannon sampling theorem for $1<Q<2$.

The Fourier transform is constructed by periodic extension, i.e., by spacing copies of the transform in a definite way, recognizing that no aliasing occurs for values of the sampling ratio such that $1<Q<2$, which can be used to advantage in the application of phase retrieval estimation. A method was developed for propagating the electromagnetic field with no aliasing, which has been extended to 2-d optical apertures.

This work was done by Bruce Dean, Jeffrey Smith, and David Aronstein of Goddard Space Flight Center. Further information is contained in a TSP (see page 1). GSC-15947-1

Space Operations Learning Center Facebook Application
This app uses the latest networking technology to inspire young audiences to be interested in math, science, and engineering.

Goddard Space Flight Center, Greenbelt, Maryland

The proposed Space Operations Learning Center (SOLC) Facebook module, initially code-named "Spaceville," is intended to be an educational online game utilizing the latest social networking technology to reach a broad audience base and inspire young audiences to be interested in math, science, and engineering.

Spaceville will be a Facebook application/game with the goal of combining learning with a fun game and social environment. The mission of the game is to build a scientific outpost on the Moon or Mars and expand the colony. Game activities include collecting resources, trading resources, completing simple science experiments, and building architectures such as laboratories, habitats, greenhouses, machine shops, etc. The player is awarded with points and achievement levels. The player's ability increases as his/her points and levels increase. A player can interact with other players using multiplayer Facebook functionality. As a result, a player can discover unexpected treasures through scientific missions, engineering, and working with others.

The player creates his/her own avatar with his/her selection of its unique appearance, and names the character. The player controls the avatar to perform activities such as collecting oxygen mole-

cules or building a habitat. From observations of other successful social online games such as Farmville and Restaurant City, a common element of these games is having eye-catching and cartoonish characters, and interesting animations for all activities. This will create a fun, educational, and rewarding environment.

The player needs to accumulate points in order to be awarded special items needed for advancing to higher levels. Trophies will be awarded to the player when certain goals are reached or tasks are completed. In order to acquire some special items needed for advancement in the game, the player will need to visit his/her neighboring towns to discover the items. This is the social aspect of the game that requires the player to go out of his/her own establishment to explore what is in the neighborhood. Spaceville will take advantage of Facebook's successful architecture to inspire a new audience of scientists and engineers for the future.

Rotorcraft Diagnostics

John H. Glenn Research Center, Cleveland, Ohio

Health management (HM) in any engineering systems requires adequate understanding about the system's functioning; a sufficient amount of monitored data; the capability to extract, analyze, and collate information; and the capability to combine understanding and information for HM-related estimation and decision-making. Rotorcraft systems are, in general, highly complex. Obtaining adequate understanding about functioning of such systems is quite difficult, because of the proprietary (restricted access) nature of their designs and dynamic models. Development of an EIM (exact inverse map) solution for rotorcraft requires a process that can overcome the above-mentioned difficulties and maximally utilize monitored information for HM facilitation via employing advanced analytic techniques.

The goal was to develop a versatile HM solution for rotorcraft for facilitation of the Condition Based Maintenance Plus (CBM+) capabilities. The effort was geared towards developing analytic and reasoning techniques, and proving the ability to embed the required capabilities on a rotorcraft platform, paving the way for implementing the solution on an aircraft-level system for consolidation and reporting.

The solution for rotorcraft can he used offboard or embedded directly onto a rotorcraft system. The envisioned solution utilizes available monitored and archived data for real-time fault detection and identification, failure precursor identification, and offline fault detection and diagnostics, health condition forecasting, optimal guided troubleshooting, and maintenance decision support. A variant of the onboard version is a self-contained hardware and software (HW+SW) package that can be embedded on rotorcraft systems.

The HM solution comprises components that gather/ingest data and information, perform information/feature extraction, analyze information in conjunction with the dependency/diagnostic model of the target system, facilitate optimal guided troubleshooting, and offer decision support for optimal maintenance.

Recursive Branching Simulated Annealing Algorithm
The algorithm can be applied to a wide variety of optimization problems.

Goddard Space Flight Center, Greenbelt, Maryland

This innovation is a variation of a simulated-annealing optimization algorithm that uses a recursive-branching structure to parallelize the search of a parameter space for the globally optimal solution to an objective. The algorithm has been demonstrated to be more effective at searching a parameter space than traditional simulated-annealing methods for a particular problem of interest, and it can readily be applied to a wide variety of optimization problems, including those with a parameter space having both discrete-value parameters (combinatorial) and continuous-variable parameters. It can take the place of a conventional simulated-annealing, Monte-Carlo, or random-walk algorithm.

In a conventional simulated-annealing (SA) algorithm, a starting configuration is randomly selected within the parameter space. The algorithm randomly selects another configuration from the parameter space and evaluates the objective function for that configuration. If the objective function value is better than the previous value, the new configuration is adopted as the new point of interest in the parameter space. If the objective function value is worse than the previous value, the new configuration may be adopted, with a probability determined by a temperature parameter, used in analogy to annealing in metals. As the optimization continues, the region of the parameter space from which new configurations can be selected shrinks, and in conjunction with lowering the annealing temperature (and thus lowering the probability for adopting configurations in parameter space with worse objective functions), the algorithm can converge on the globally optimal configuration.

The Recursive Branching Simulated Annealing (RBSA) algorithm shares some features with the SA algorithm, notably in-

cluding the basic principles that a starting configuration is randomly selected from within the parameter space, the algorithm tests other configurations with the goal of finding the globally optimal solution, and the region from which new configurations can be selected shrinks as the search continues. The key difference between these algorithms is that in the SA algorithm, a single path, or trajectory, is taken in parameter space, from the starting point to the globally optimal solution, while in the RBSA algorithm, many trajectories are taken; by exploring multiple regions of the parameter space simultane-

ously, the algorithm has been shown to converge on the globally optimal solution about an order of magnitude faster than when using conventional algorithms.

Novel features of the RBSA algorithm include:
1. More efficient searching of the parameter space due to the branching structure, in which multiple random configurations are generated and multiple promising regions of the parameter space are explored;
2. The implementation of a trust region for each parameter in the parameter space, which provides a natural way of

enforcing upper- and lower-bound constraints on the parameters; and
3. The optional use of a constrained gradient-search optimization, performed on the continuous variables around each branch's configuration in parameter space to improve search efficiency by allowing for fast fine-tuning of the continuous variables within the trust region at that configuration point.

This work was done by Matthew Bolcar, J. Scott Smith, and David Aronstein of Goddard Space Flight Center. Further information is contained in a TSP (see page 1). GSC-15908-1

❯ Method for Pre-Conditioning a Measured Surface Height Map for Model Validation

This method can be implemented in most optical modeling and simulation software.

NASA's Jet Propulsion Laboratory, Pasadena, California

This software allows one to up-sample or down-sample a measured surface map for model validation, not only without introducing any re-sampling errors, but also eliminating the existing measurement noise and measurement errors. Because the re-sampling of a surface map is accomplished based on the analytical expressions of Zernike-polynomials and a power spectral density model, such re-sampling does not introduce any aliasing and interpolation errors as is done by the conventional interpolation and FFT-based (fast-Fourier-transform-based) spatial-filtering method. Also, this new method automatically eliminates the measurement noise and other measurement errors such as artificial discontinuity.

The developmental cycle of an optical system, such as a space telescope, includes, but is not limited to, the following two steps: (1) deriving requirements or specs on the optical quality of individual optics before they are fabricated through optical modeling and simulations, and (2) validating the optical model using the measured surface

height maps after all optics are fabricated. There are a number of computational issues related to model validation, one of which is the "pre-conditioning" or pre-processing of the measured surface maps before using them in a model validation software tool.

This software addresses the following issues: (1) up- or down-sampling a measured surface map to match it with the gridded data format of a model validation tool, and (2) eliminating the surface measurement noise or measurement errors such that the resulted surface height map is continuous or smoothly-varying. So far, the preferred method used for re-sampling a surface map is two-dimensional interpolation. The main problem of this method is that the same pixel can take different values when the method of interpolation is changed among the different methods such as the "nearest," "linear," "cubic," and "spline" fitting in Matlab. The conventional, FFT-based spatial filtering method used to eliminate the surface measurement noise or measurement errors can also suffer from aliasing effects.

During re-sampling of a surface map, this software preserves the low spatial-frequency characteristic of a given surface map through the use of Zernike-polynomial fit coefficients, and maintains mid- and high-spatial-frequency characteristics of the given surface map by the use of a PSD model derived from the two-dimensional PSD data of the mid- and high-spatial-frequency components of the original surface map. Because this new method creates the new surface map in the desired sampling format from analytical expressions only, it does not encounter any aliasing effects and does not cause any discontinuity in the resultant surface map.

This work was done by Erkin Sidick of Caltech for NASA's Jet Propulsion Laboratory. Further information is contained in a TSP (see page 1).

The software used in this innovation is available for commercial licensing. Please contact Daniel Broderick of the California Institute of Technology at danielb@caltech.edu. Refer to NPO-47593.

Books & Reports

***In Situ* Potassium-Argon Geochronology Using Fluxed Fusion and a Double Spike**

A document highlights an Li-based fluxing agent that enables sample fusion and quantitative Ar-release at relatively low temperatures (900–1,000 ºC), readily achievable with current flight resistance furnace designs. A solid, double spike containing known quantities of ^{39}Ar and ^{41}K was developed that, when added in known amounts to a sample, enables the extraction of a ^{40}Ar/^{40}K ratio for age estimation without a sample mass measurement.

The use of a combination of a flux and a double spike as a means of solving the mechanical hurdles to an *in situ* K-Ar geochronology measurement has never been proposed before. This methodology and instrument design would provide a capability for assessing the ages of rocks and minerals on the surfaces of planets and other rocky terrestrial bodies in the solar system.

This work was done by Joel A. Hurowitz, Michael H. Hecht, Wayne F. Zimmerman, Evan L. Neidholdt, Mahadeva P. Sinha, Wolfgang Sturhahn, Max Coleman, Daniel J. McCleese, Kenneth A. Farley, John M. Eiler, and George R. Rossman of Caltech, and Kathryn Waltenberg of the University of Queensland, Australia, for NASA's Jet Propulsion Laboratory. Further information is contained in a TSP (see page 1). NPO-48099

⊚ **Fiber-Optic Micrometeoroid/Orbital Debris Impact Detector System**

A document describes a reliable, lightweight micrometeoroid/orbital debris (MMOD) detection system that can be located at strategic positions of "high consequence" to provide real-time warning of a penetration, its location, and the extent of the damage to a spacecraft.

The concept is to employ fiber-optic sensors to detect impact damage and penetration of spacecraft structures. The fibers are non-electrical, employ light waves, and are immune to electromagnetic interference.

The fiber-optic sensor array can be made as a standalone product, being bonded to a flexible membrane material

or a structure that is employed as a MMOD shield material. The optical sensors can also be woven into hybrid MMOD shielding fabrics. The glass fibers of the fiber-optic sensor provide a dual purpose in contributing to the breakup of MMOD projectiles. The grid arrays can be made in a modular configuration to provide coverage over any area desired. Each module can be connected to a central scanner instrument and be interrogated in a continuous or periodic mode.

This work was done by Eric L. Christiansen of Johnson Space Center and R.C. Tennyson and W.D. Morison of Fiber Optic Systems Technology Inc. (FOX-TEK). Further information is contained in a TSP (see page 1).

In accordance with Public Law 96-517, the contractor has elected to retain title to this invention. Inquiries concerning rights for its commercial use should be addressed to:

Fiber Optic Systems Technology Inc.
4580 Dufferin St. Suite 402
Toronto, Ontario, Canada M3H 5Y2
Refer to MSC-23934-1, volume and number of this NASA Tech Briefs *issue, and the page number.*

⊚ **Nanostructure Secondary-Mirror Apodizing Mask for Transmitter Signal Suppression in a Duplex Telescope**

A document discusses a nanostructure apodizing mask, made of multi-walled carbon nanotubes, that is applied to the centers (or in and around the holes) of the secondary mirrors of telescopes that are used to interferometrically measure the strain of space-time in response to gravitational waves. The shape of this ultra-black mask can be adjusted to provide a smooth transition to the clear aperture of the secondary mirror to minimize diffracted light.

Carbon nanotubes grown on silicon are a viable telescope mirror substrate, and can absorb significantly more light than other black treatments. The hemispherical reflectance of multi-walled carbon nanotubes grown at GSFC is approximately 3 to 10 times better than a standard aerospace paint used for stray light control. At the LISA (Laser Interferometer Space Antenna) wavelength of 1 micron, the advantage over paint is a factor of 10.

Primarily, in the center of the secondary mirror (in the region of central obscu-

ration, where no received light is lost) a black mask is applied to absorb transmitted light that could be reflected back into the receiver. In the LISA telescope, this is in the center couple of millimeters. The shape of this absorber is critical to suppress diffraction at the edge. By using the correct shape, the stray light can be reduced by approximately 10 to the 9 orders of magnitude versus no center mask. The effect of the nanotubes has been simulated in a stray-light model. The effect of the apodizing mask has been simulated in a near-field diffraction model. Specifications are geometry-dependent, but the baseline design for the LISA telescope has been modeled as well. The coatings are somewhat fragile, but work is continuing to enhance adhesion.

This work was done by John Hagopian, Jeffrey Livas, Shahram Shiri, Stephanie Getty, June Tveekrem, and James Butler of Goddard Space Flight Center. Further information is contained in a TSP (see page 1). GSC-16029-1

⊚ **Advanced Fire Detector for Space Applications**

A document discusses an optical carbon monoxide sensor for early fire detection. During the sensor development, a concept was implemented to allow reliable carbon monoxide detection in the presence of interfering absorption signals.

Methane interference is present in the operating wavelength range of the developed prototype sensor for carbon monoxide detection. The operating parameters of the prototype sensor have been optimized so that interference with methane is minimized. In addition, simultaneous measurement of methane is implemented, and the instrument automatically corrects the carbon monoxide signal at high methane concentrations. This is possible because VCSELs (vertical cavity surface emitting lasers) with extended current tuning capabilities are implemented in the optical device. The tuning capabilities of these new laser sources are sufficient to cover the wavelength range of several absorption lines. The delivered carbon monoxide sensor (COMA 1) reliably measures low carbon monoxide levels even in the presence of high methane signals. The signal bleed-over is determined during system calibration and is then accounted for in the system parameters.
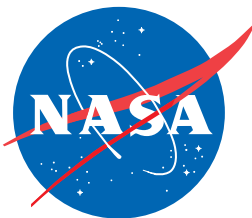
The sensor reports carbon monoxide concentrations reliably for (interfering) methane concentrations up to several thousand parts per million.

This work was done by Joerg Kutzner of Vista Photonics, Inc. for Glenn Research Cen- *ter. Further information is contained in a TSP (see page 1).*

Inquiries concerning rights for the commercial use of this invention should be addressed to NASA Glenn Research Center, Innovative Partnerships Office, Attn: Steven Fedor, Mail *Stop 4–8, 21000 Brookpark Road, Cleveland, Ohio 44135. Refer to LEW-18783-1*

National Aeronautics and
Space Administration